2 mil

SPERRY
FLIGHT SYSTEMS

PHOENIX, ARIZONA 85036

FINAL REPORT
DESIGN STUDY FOR A MAGNETICALLY SUPPORTED REACTION WHEEL

CONTRACT NO. 953884 WITH JPL

This work was performed for the Jet Propulsion Laboratory, California Institute of Technology sponsored by the National Aeronautics and Space Administration under Contract NAS7-100.

PREPARED BY

G. STOCKING

J. DENDY

A. SABNIS

APPROVED BY

J. R. DOHOGNE

SPERRY
FLIGHT SYSTEMS

PHOENIX, ARIZONA

COPY NO._____

PRINTED IN U.S.A. JULY 1974 PUB. NO. 71-0489-00-00

ABSTRACT

This report describes the results of a study program in which the characteristics of a magnetically supported reaction wheel are defined. Tradeoff analyses are presented for the principal components, which are then combined in several reaction wheel design concepts. A preliminary layout of the preferred configuration is presented, along with calculated design and performance parameters. Recommendations are made for a prototype development program.

TABLE OF CONTENTS

GLOSSARY

Z = Displacement Coordinate (in.)

M = Mass (lb sec^2/ft)

K = Stiffness (lb/in., in.-lb/rad)

F = Force (lb)

B = Damping Coefficient or Flux Density (Webers/$meter^2$)

t = Time (sec)

k = Electronic or Servo Gain Factor

W = Weight (lb)

I = Moment of Inertia (ft-lb-sec^2)

H = Angular Momentum (ft-lb-sec)

ω = Angular Velocity (rad/sec)

N = Angular Velocity (rpm)

R = Rotor Radius (in.)

η, ϵ = Motor Efficiencies

T = Torque or Tooth Width (in.)

P = Power (w)

g = Gravitational Constant or Axial Gap (ft/sec^2, in.)

f = Frequency (rad/sec)

ℓ = Axial Bearing Span (in.)

Ω = Cross Axis Rate Input (rad/sec)

α = Angle or Equation Coefficient

r = Radius of Magnetic Bearing Rings (in.)

SUMMARY

This report describes the results of a preliminary design study program conducted to determine the feasibility of the use of magnetic bearings in a reaction wheel for interplanetary and orbiting spacecraft. The resulting design met or exceeded all the design objectives, and is competitive with ball bearing designs in terms of weight and power. Additionally, it provides virtually unlimited life, and does not require any basic new technology developments. All the concepts incorporated in this design have been used operationally or, in the case of the magnetic suspension, demonstrated in operational hardware.

An outline drawing is shown in Figure i-1. The major parameters are listed in the table below.

Parameter	Design Objective	Attained Value
Angular Momentum	±.5 ft-lb-sec	±.5 ft-lb-sec
Weight	8.0 lb	6.52 lb
Volume	250 $in.^3$	220 $in.^3$
Cross Axis Rate (maximum)	17.5 mr/sec	832 mr/sec
Output Torque (minimum)	.01 ft/lb	.01 ft/lb
Max Motor Power	8 watts	8 watts
Bearing Power		
Maximum	8 watts	8 watts
Average	1 watt	.5 watt

The design has intergral suspension electronics and utilizes a unique segmented spin motor design which permits the incorporation of a redundant spin motor stator. It utilizes a passive radial magnetic bearing configuration which does not require close manufacturing tolerances and is capable of being operated and adjusted prior to assembly into the unit. The rotational drag associated with the magnetic suspension system is .015 oz-in. at 1500 rpm (.06 watt).

It is significant to note that the RWA design offers the potential of no single point failures in one mechanical device, which is achieved simply by providing redundant electronics; the additional weight required to achieve this goal is .4 pound. The reliability of the RWA without redundant bearing electronics

.s .913 for the 10-year life, and the addition of redundant electronics will .ncrease this to .994 for 10 years. Adding a redundant spin motor increases the :otal RWA reliability to .996, at the expense of an additional .6 pound.

Parameter variations are readily achieved within the same physical dimen-;ions. The sensitivity of the design to peak motor power is a .30 pound/watt and :o momentum is 2.4 pound/foot-pound-second. Thus a .5 foot-pound-second design ;ith 4 watts maximum spin motor power would weigh 7.72 pounds. Similar scalings :an be made for other values of angular momentum.

The outline drawing in Figure i-1 illustrates a flat base mounting tech-ıique. Several variations of this are possible depending on the vehicle in which .t is being used. A cg mount would reduce the weight and provide a more optimum ıotor segment mounting scheme. The configuration provides ample room for inte-;ral mounting of the suspension and spin motor drive electronics. The concept of :limination of the cover can be considered since there is no lubricant to con-:ain, and the only path for particle contamination would be through the motor ;ap. This approach could represent a 1.0 to 1.5 pound weight saving.

The cost of a magnetically suspended reaction wheel is comparable to that of ı ball bearing unit. The addition of the suspension electronics is offset by the :eduction in the number of parts, and also by the absence of close tolerance ıachining.

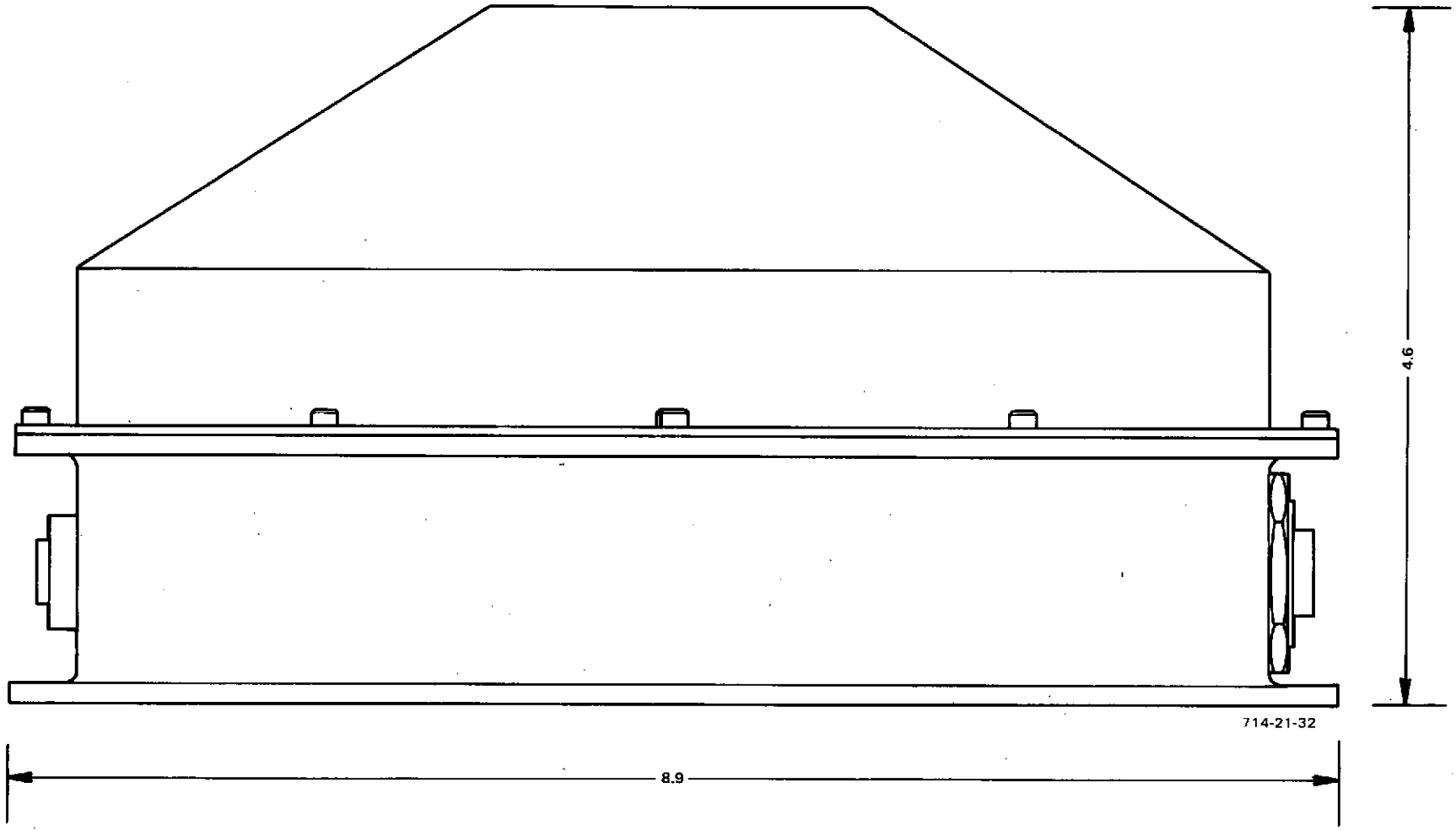

Figure 1-1
Reaction Wheel Assembly Outline Drawing

SECTION 1.0

INTRODUCTION

SECTION 1.0

INTRODUCTION

This report is submitted in partial fulfillment of JPL Contract 953884, "Long Life Magnetic Bearing Reaction Wheel Study". It is the final report, and contains all technical information developed during the course of the design study.

1.1 BACKGROUND

The use of Reaction Wheel Assemblies (RWA) is a proven and accepted technique for precise control of spacecraft attitude. In a typical system, three orthogonally mounted RWAs are employed, each developing bi-directional control torques about a spacecraft axis in response to commands from the attitude control sensors. Redundancy can be achieved by the addition of a fourth RWA, whose spin axis is skewed to the other three RWAs.

The total momentum exchange system can be configured as having a nominal zero bias, or else can have a finite momentum at all times along a particular spacecraft axis. In the case of a zero bias system, which is of particular interest here, the RWAs must be capable of operation in both directions of rotation, including the region about zero speed. Although ball bearing supported wheels have achieved lifetimes in the neighborhood of 4 to 5 years, their use for 10 year interplanetary missions, as required in this design study, is highly questionable. The central reason for this is the necessity of assuring the presence of a lubricant in the ball contact area over this period of time, and of providing a load carrying film (or boundary lubrication) in the near zero speed region. Also, while statistical proof of long life can be accomplished on a design basis for a ball bearing system, it is virtually impossible to guarantee its existence on each individual RWA.

The obvious solution to the ball bearing problem is to avoid metal-to-metal contact of the bearing elements, and to eliminate the need for a lubricant supply. Magnetic bearings constitute such a contactless support system, and form the basis for the RWA design study described in this report.

1.2 TECHNICAL APPROACH

The objective of this study is to characterize the design of a long life (10 years) RWA with magnetic bearings to determine the feasibility for use in interplanetary spacecraft. In particular, the size, weight and power parameters of the RWA are defined for the specified performance and operational requirements. In order to accomplish the above objectives, the RWA was considered in terms of six major functional elements:

- Inertia Element
- Spin Motor
- Magnetic Bearing System
- Bearing Control Electronics
- Housing Structure
- Touchdown System

The above items were defined as components of the RWA, each subject to its own constraints (e.g., maximum spin motor power). The overall design approach was selected from several conceptual layouts prepared from various combinations of these elements. A preliminary RWA layout and description was then prepared for the most desirable design approach.

The starting point for the magnetic bearing design was an existing Sperry three-loop design, which is described in Appendix A of this report. A previously developed variation of this design, termed a one-loop bearing is also considered for use in the RWA design.

Section 2.0 contains a general discussion of magnetic bearings, and presents the rationale for selection of the specific type for RWA designs. The technical description of the RWA design is presented in Section 3.0.

Conclusions of the study are presented in Section 4.0, and include a discussion of the incorporation of total redundancy in a single RWA. Recommendations for further development effort are contained in Section 5.0.

SECTION 2.0

MAGNETIC BEARING TYPE SELECTION

SECTION 2.0

MAGNETIC BEARING TYPE SELECTION

Magnetic bearings can be configured in many different ways, depending upon the equipment design and performance requirements. This section presents an approach to magnetic bearing classification and develops the rationale for the selection of the specific type selected for use in spacecraft reaction wheels.

2.1 MAGNETIC BEARING CHARACTERISTICS

Magnetic suspension offers many advantages for rotational equipment, but as may be expected, some limitations are also incurred. A summary of these characteristics is presented in Table 2-1.

TABLE 2-1

MAGNETIC BEARING CHARACTERISTICS

ADVANTAGES
• High reliability (no wear, lubrication or fatigue)
• Low torque (starting, drag and ripple)
• High speed capability
• Low noise and vibration
• No single point failures (with redundant electronics)
• Compatible with vacuum environment (no lubricant)
• Insensitive to thermal conditions (large gaps)
LIMITATIONS
• Lower load capacity per unit weight
• Control electronics required

The advantages arise from the basic nature of contactless suspension (non-bearing). High reliability is possible because of the elimination of the lubrication, wear and fatigue characteristics normally associated with ball or fluid bearings; however, a control system must be provided, and its failure rate must be accounted for in the reliability calculation. In connection with this point, it is of interest to note that redundancy can easily be incorporated in the

control system electronics; thus, single point failures can be eliminated in the entire RWA system without duplication of the mechanical and structural elements (rotor, housing, etc).

The limitation of lower load carrying capacity is a result of the physics of magnetic force generation: a pair of magnetized surfaces can develop a load capability of 232 psi at a flux level of 20,000 gauss (near saturation level for iron). When compared with the 300,000 psi design limit for ball bearing steels, it can be appreciated that substantially more material must be provided to obtain the same total bearing capacity. In order to minimize total system weight, it is therefore very important to design the bearings for the minimum required capacity and/or stiffness.

2.2 CLASSIFICATION OF MAGNETIC BEARINGS

Magnetic bearings can, in general, be placed in three categories:

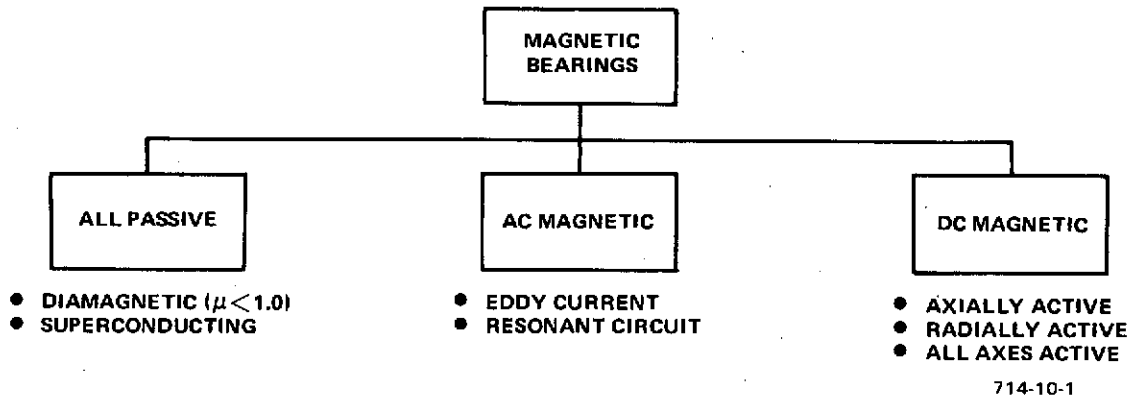

All-passive systems are not subject to the constraints of Earnshaw's theorem (as discussed in the following paragraph) and thus do not require an active control system to achieve 3-dimensional stability. However, diamagnetic materials have very low load capacity per unit weight because the permeability of diamagnetic materials is very close to 1 (e.g., bismuth = .99). Superconducting bearing systems require the added weight and complexity of a cooling system. Thus, all-passive bearings are not viable candidates for space equipment.

Earnshaw's theorem states the conditions for instability in magnetostatic, inverse square fields. Its practical consequence, as applied to paramagnetic materials ($\mu > 1.0$), is that external stabilizing means must be provided in at

least one coordinate direction. Suitable time-varying fields must therefore be employed in ac and dc magnetic systems to obtain completely contactless suspension.

The ac systems, both eddy-current and resonant, are characterized by high power loss and poor damping characteristics. For the RWA application, therefore, the choice can be narrowed to one of the dc systems. Selection of the specific type of dc system is discussed in the following paragraph.

2.3 COMPARISON OF DC MAGNETIC BEARING TYPES

DC magnetic bearings were first so termed because a steady-state current was used to provide passive magnetic restoring forces, with modulation of this current used to provide total (3-dimensional) stability and levitation. This category has since been extended to include bearings in which the passive restoring forces are provided by permanent magnets rather than by electromagnets. Rotational dc magnetic bearings may be divided into three classes:

- Axial active, radial passive (1 degree-of-freedom is actively controlled)
- Radial active, axial passive (4 degrees-of-freedom are actively controlled)
- All-active (5 degrees-of-freedom are actively controlled)

The comparative characteristics of the three types of systems are summarized in Table 2-2.

TABLE 2-2

PROPERTIES OF DC MAGNETIC BEARINGS

Characteristics	Type		
	Axial Active - Radial Passive	Radial Active - Axial Passive	All Axes Active
Stiffness			
Radial	Low	Adjustable	Adjustable
Axial	Adjustable	Low	Adjustable
Bearing Torque	Lowest	Low	Low
Power Loss	Low	High	High
Control System	1 degree-of-freedom	4 degrees-of-freedom	5 degrees-of-freedom
Reliability	High	Low	Lowest

The principal advantage of using passive means to obtain restoring forces is inherent simplicity and reliability; neither sensors, electronics, nor control coils are required. When the quiescent field used to obtain the passive restoring forces is provided by permanent magnets, the power losses due to steady coil currents are eliminated. However, the bearing stiffness is entirely determined by the passive magnetics and, unless separate means are provided, cannot be altered from the original value. Additional damping forces (e.g., from eddy-currents) must be provided in order to ensure satisfactory dynamic response and well-bounded amplitudes at resonant conditions.

Active means of obtaining magnetic support forces have the advantages of adjustable stiffness and damping characteristics, which are obtainable by variation of control system parameters. The disadvantages are that sensors, electronics, and forcing coils are required, with a resultant lowering of reliability. Moreover, an active system requires suspension power not only during dynamic-load conditions, but also standby electronics power during static-load conditions.

Selection of a particular bearing type depends heavily on application requirements; in fact, models of each type have been constructed at one time by various manufacturers. In one important area - reliability - the axially active/radially passive bearing is superior to the other types. The reason for this is the number of degrees-of-freedom required in the control system. When active radial control is employed, two angular modes are introduced in addition to the two

radial modes, for a total of four control axes. While this is not necessarily prohibitive in itself, the incorporation of monitoring and redundancy techniques is extremely complex. Thus, it is primarily for the reliability consideration that the active axial-passive radial type bearing was chosen for reaction wheels. It should be noted, however, that, for the same radial stiffness, the weight of this type bearing is likely to be higher than for an active bearing, and that specific attention must be directed to designing for the minimum allowable radial spring rate for each application.

Consideration is now given to the nature of the passive-radial suspension and to the method of axial control force generation for this type of bearing.

2.4 REPULSION VERSUS ATTRACTION

Schematic illustrations of passive repulsion and attraction suspension techniques are shown in Figures 2-1 and 2-2, along with a listing of advantages and disadvantages. In the repulsion system, the radial restoring force is generated by the reaction between like magnetic poles. In the attraction system, the radial restoring force is caused by the tendency of the rotor to be in a position of minimum reluctance of the magnetic circuit.

In comparing the relative merits of these techniques, two significant factors can be noted:

- The flux is contained within the magnetic circuit in the attraction bearing, but is forced to be external in the repulsive bearing. This flux containment results in reduced bearing drag torques, and also minimizes unwanted vehicle disturbance torques that would otherwise be generated by interaction with nearly magnetic fields and components.

- In the repulsion bearing, a separate means (such as a dual-acting solenoid) must be provided to generate bi-directional axial control forces; in the attractive bearing, it is possible to modulate (increase or decrease) the existing magnetic field to generate axial control forces. For minimum standby power, the solenoids are excited separately; the resulting axial control force is proportional to the square of flux density $(B_o)^2$. When an existing bias field is modulated, however, the control force is proportional to $B_o \Delta B$, where

- ADVANTAGES
  - LOWER UNBALANCE STIFFNESS RATIO ($K_U/K_R \approx -2$)
- DISADVANTAGES
  - STRAY FIELDS
    - HIGHER DRAG TORQUES
    - INTERACTION WITH ADJACENT COMPONENTS
  - SEPARATE AXIAL CONTROL TECHNIQUE REQUIRED
  - LOWER CAPACITY
  - MAGNETS ON SHAFT
    - SPEED LIMITATION

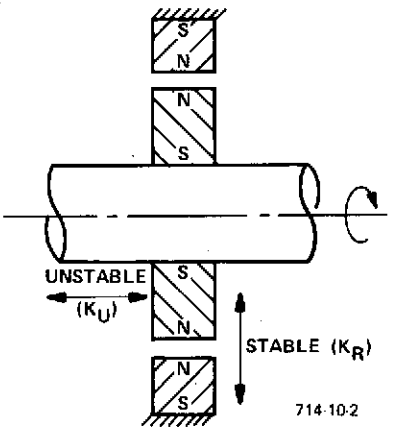

Figure 2-1
Passive Radial Suspension, Repulsion

- RESTORING FORCE DUE TO VARIATION OF RELUCTANCE
- ADVANTAGES
  - CONTAINED FIELDS
  - FIELD MODULATION FOR AXIAL CONTROL
  - HIGHER CAPACITY
  - MAGNETS STATIONARY
- DISADVANTAGES
  - HIGHER UNBALANCE STIFFNESS RATIO ($K_U/K_R \approx -8$)
  - COIL MUST OVERCOME MAGNET RELUCTANCE

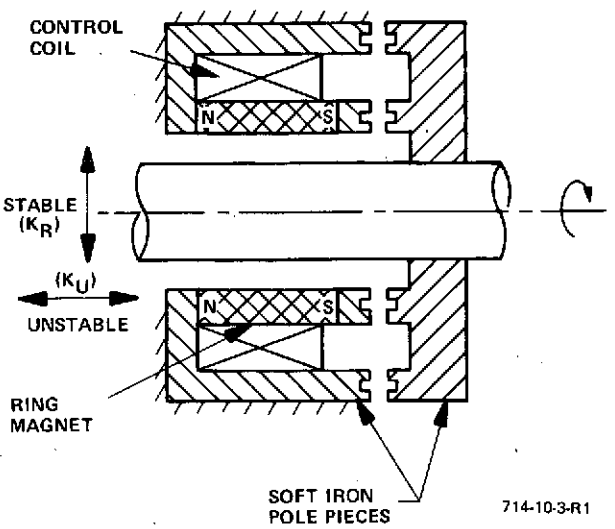

Figure 2-2
Passive Radial Suspension, Attraction

ΔB is produced by the coil; thus the force is linear and takes on, as a gain factor, the quiescent flux density (B_o) established by the permanent magnet system.

A comparison of the other features listed in Figures 2-1 and 2-2 also favors the attractive system. The disadvantage of higher unbalance stiffness ratio could necessitate a higher initial lift-off coil current which, however, is a short term transient.

To summarize, the preferred bearing for spacecraft reaction wheels:

- Is dc magnetic
- Is active-axial, passive-radial
- Uses an attractive magnetic circuit

2.5 CONTROL CONCEPTS FOR THE ACTIVE AXIS

As a consequence of Earnshaw's theorem, the radial restoring stiffness of the passive magnetics is accompanied by instability in the axial direction. Because this unbalance force is a function of the difference between the squares of two terms, the net force in the axial direction is a linear function of axial displacement near the equilibrium position. The axial equation of motion of the magnetic suspension is therefore given by

$$M \ddot{z} - K_u z = F$$

where

z = axial displacement from the equilibrium position

M = suspended mass

K_u = unbalance stiffness

F = applied force (total)

Axial stability can be obtained by controlling the current to the control coils to generate forces in the proper direction. Thus, if the control force includes rate-plus-displacement feedback given by

$$F_c = -B \dot{z} - K z,$$

then the axial equation of motion becomes

$$M \ddot{z} + B \dot{z} + (K - K_u) z = F_e$$

where F_e is the external force. This equation indicates system stability can be obtained for $K > K_u$, a net static stiffness of $(K - K_u)$ and resultant power loss under external axial loads. In practice, the rate sensor may be avoided by using lead compensation of the position signal. A block diagram of the axial control system is shown in Figure 2-3, and the root locus in Figure 2-4.

In addition to the lead compensation, a minor loop integrator can be added (shown by dashed lines in Figure 2-3), in order that the unbalance stiffness of the passive magnetics can be used to advantage in overcoming external loads. The integrator also enables long-term, low-power operation by correcting for drift in any of the electronic components, including the position sensor. With integral feedback, the static axial stiffness is negative; the root locus of this system is shown in Figure 2-5.

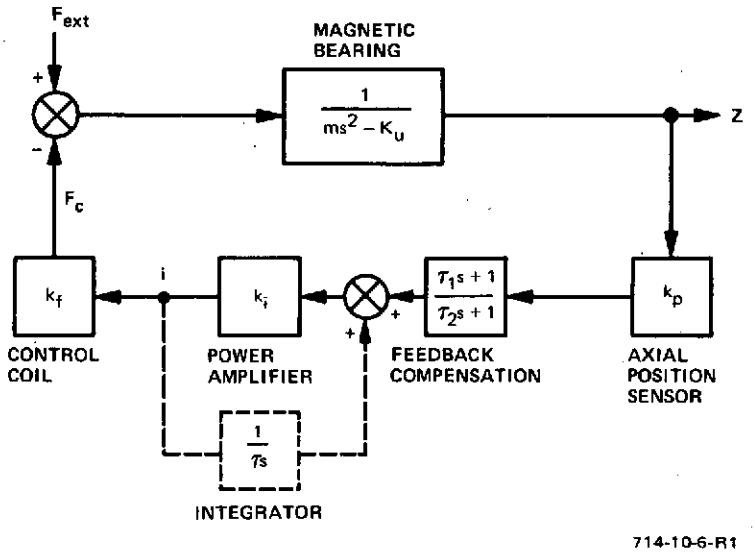

Figure 2-3
Axial Control System Block Diagram

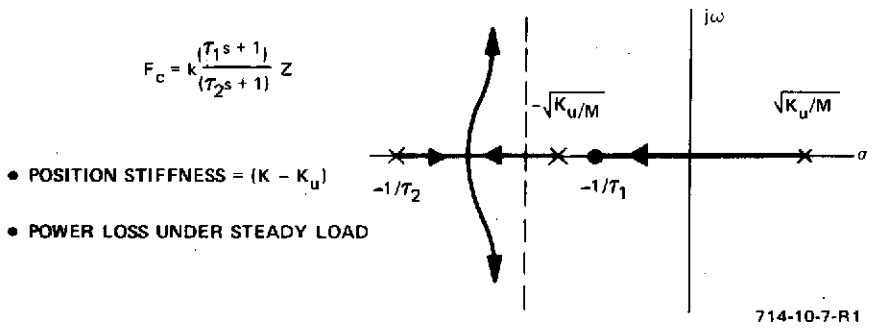

Figure 2-4
Root Locus, Lead Compensation

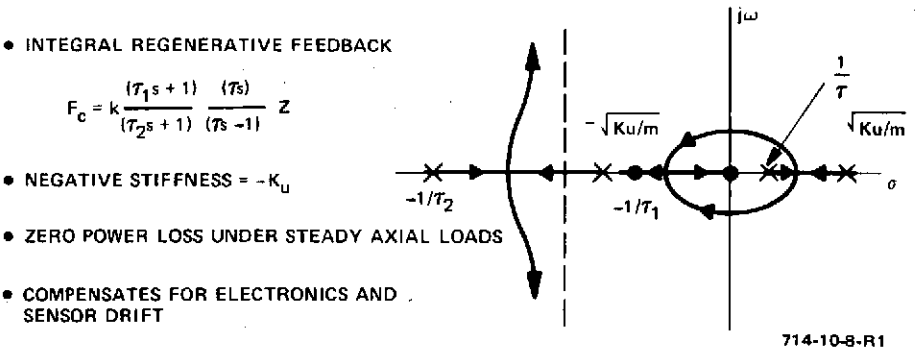

Figure 2-5
Root Locus, Integral Feedback

SECTION 3.0

REACTION WHEEL DESIGN

SECTION 3.0

REACTION WHEEL DESIGN

This section presents a discussion of the design tradeoffs leading to a preferred configuration for a magnetically suspended RWA. The design objectives are interpreted in terms of RWA requirements, and specific component analyses are developed. Conceptual RWA design approaches are compared and evaluated. A preliminary RWA layout is presented for the preferred approach, along with calculated design and performance parameters.

3.1 RWA DESIGN OBJECTIVES

The design specifications for the RWA are listed in Table 3-1. Those which have the most influence on the design tradeoffs are listed separately as primary specifications.

TABLE 3-1

RWA SPECIFICATIONS

PRIMARY DESIGN OBJECTIVES

Angular Momentum	+.5 to -.5 ft-lb-sec
Motor Torque (minimum)	-.01 to +.01 vt-lb
Motor Power (maximum)	8 watts
Bearing System Power (maximum)	8 watts (peak)
	1 watt (average)
Cross Axis Rate (maximum)	.0175 radian/second
Weight (maximum)	8 pounds
Volume (maximum)	250 $inch^3$
Temperature Range	+20°C to +75°C
Pressure (ambient)	10^{-14} torr
Life (minimum)	10 years, operating
Shock and Vibration	TBD

TABLE 3-1 (cont)

RWA SPECIFICATIONS

SECONDARY DESIGN OBJECTIVES

Radial Magnetic Field (maximum	10 nanotesla (10^{-4} gauss) at 1 meter
Radial Magnetic Field Variation	4 nanotesla at 1 meter, 0 to 30 Hz
Radiation Resistance	10^4 rads (silicon)
Bearing System Stiffness (nominal)	
Radial (total)	330 lb/in
Axial	2000 lb/in
Bearing System Capacity (nominal)	
Radial (total)	7 pounds
Axial	25 pounds

The motor torque is the net (accelerating/decelerating) torque applied to the wheel, and its reaction is useable for vehicle control purposes. This torque must be delivered upon command in either direction over the total angular momentum range of the wheel. The maximum motor power of 8 watts includes that required for bearing and windage drag, in addition to the net torque delivered to the vehicle.

The cross axis rate input causes a deflection at each bearing due to gyroscopic effects ($\overline{\omega} \times \overline{H}$). The interpretation of this requirement is that there be no physical contact of the touchdown bearing elements during this condition.

The weight and volume requirements include the RWA plus one channel of bearing control electronics. Spin motor control electronics and/or redundant bearing control electronics are items for separate consideration.

Meeting the performance requirements at low ambient pressure and over the stated temperature range should not be a problem as it is with ball bearing wheels. Because magnetic bearings are low power devices and are directly compatible with hard vacuum, the housing can be vented directly to space with no adverse effects on the RWA. Performance over the temperature range should also be readily achieved because of the absence of lubricants, and in fact, can be expected to show no substantial variation from standard test conditions.

The 10 year life requirement does not apply in the normal mechanical sense because wearout mechanisms are not present. Thus, the definition of life is reduced to determining the reliability of the magnetic bearing control system based on constant failure rates. Redundancy, along with improved reliability, can be achieved by duplication of the electronics to operate on a standby basis.

The external radial fields are difficult to assess analytically, and also require a very sophisticated setup for measurement. (The earth's magnetic field is approximately 50,000 nanoteslas.) The implication of this requirement in the RWA design is to contain the fields and use opposing polarities in the magnetic bearings, and to use non-magnetic materials whenever possible elsewhere.

The bearing system stiffness and capacities listed are actually those of Sperry model bearing (Appendix A), and do not necessarily have a direct relationship to the RWA design. The radial stiffness and capacity requirements are established by the angular stiffness required to sustain $\overline{\omega} \times \overline{H}$ torque loading by rotor-bearing dynamics considerations and/or 1-g operation. Axial stiffness and capacity are somewhat arbitrary within broad limits, and can be set to a desired value by adjusting the servo gain.

3.2 COMPONENT ANALYSES

3.2.1 Inertia Element

For purposes of RWA optimization, which is defined as minimum weight, it is necessary to characterize the total weight of the rotating elements in terms of the radius of the rotor rim and rotor speed, considering the rotor to consist of a rim attached by a web to a shaft on bearings. To develop the required relationship, start by defining the ratios

$$\overline{I} = \frac{I_{rim}}{I_R} \tag{3-1}$$

$$\overline{W} = \frac{W_{rim}}{W_R} \tag{3-2}$$

where

I_{rim} = inertia of rotor rim

I_R = total inertia of rotating elements

W_{rim} = weight of rotor rim

W_R = total weight of rotating elements

Also, the inertia of the rim, considered as a thin hoop, is

$$I_R = \frac{W_{rim}}{g} R^2 \tag{3-3}$$

where

R = rotor radius

The angular momentum (H) is given by

$$H = I_R \frac{2\pi N}{60} \tag{3-4}$$

where

N = rotor speed (rpm)

Substituting Equations (3-1), (3-2) and (3-3) into (3-4) and rearranging yields

$$W_R = \frac{60\ g\ H}{2\pi\ NR^2} \frac{(\bar{I})}{(\bar{W})} \tag{3-5}$$

The ratio $(\bar{I})/(\bar{W})$ varies with the size and construction of the rotor. In the size range of interest, a representative value can be taken as .6. For the nominal angular momentum H = .5 ft-lb-sec,

$$W_R = \frac{36860}{NR^2} \tag{3-6}$$

where the units are pounds (W_R), rpm (N) and inches (R). A plot of Equation (3-6) is presented in Figure 3-1, with R treated as a parameter.

In determining the range of rotor radii and rpm, the following constraints must be considered:

o Power-Limited Speed

For the case where maximum motor power and required RWA torque are specified, the rpm is constrained by

$$N_{max} \leq 1352 \frac{\eta}{T} P \tag{3-7}$$

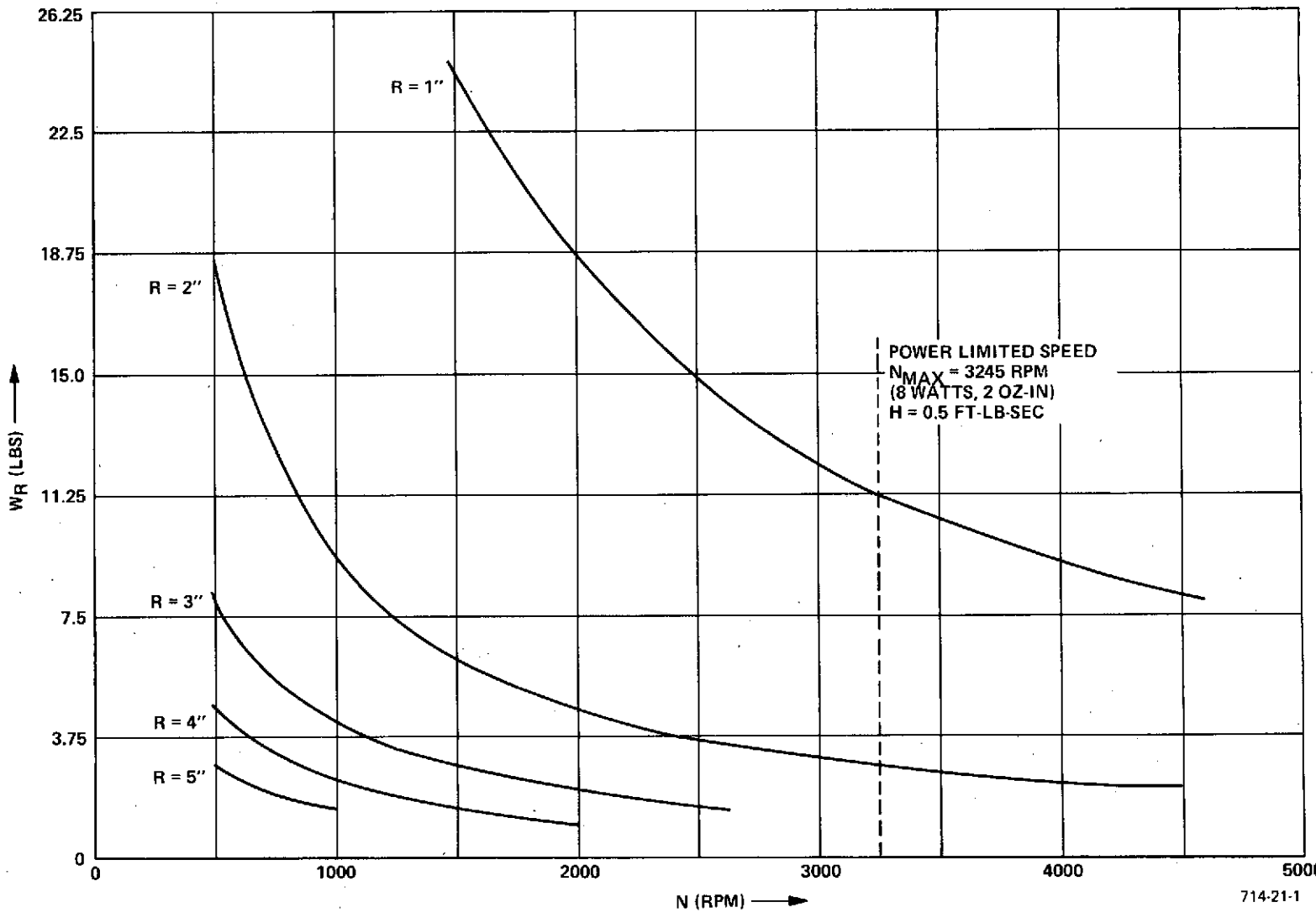

Figure 3-1
Total Rotor Weight (W_R) versus Speed (N), H = .5 foot-pound-second

where

η = motor efficiency at N_{max}

P = maximum motor power (watts)

T = motor output torque at N_{max} (oz-in)

The specified torque is .01 ft-lb = 1.92 oz-in. With allowance for the additional torque due to magnetic bearing drag, T = 2 oz-in can be used for P = 8 watts; therfore

$$N_{max} \leq 5408\ \eta \tag{3-8}$$

Thus the theoretical maximum rpm that can be considered for the design, corresponding to $\eta = 1$, is 5408 rpm. The practical limit, using an efficiency for an ac induction motor of $\eta = .6$, is 3245 rpm. This constraint is shown in the curves of Figure 3-1.

- Minimum Rotor Weight

  The minimum rotor weight must at least equal the sum of the motor cage, shaft and magnetic bearing rotors. In this case $\overline{W} = 0$, $\overline{I} = 0$ and Equation 3-6 does not apply. This constraint is dependent upon the design approach taken for the rotor, and is examined in each individual case.

- Rim Size

  The rim weight and cross-section decreases rapidly with increasing speed and increasing radius. Thus, once an optimal design is determined, it is necessary to provide sufficient cross-sectional area in the rim for the required rotor weight. This can be accomplished by material selection and/or variation of the aspect ratio of the trim cross-sectional area.

3.2.2 Spin Motor

The selection of a spin motor for a low angular momentum reaction wheel is very dependent on the overall design concept of the unit. For this study the effort was limited to ac induction type spin motors, based on the fact that they have the highest efficiency of ac devices, and the failure rate of the motor control system is approximately one-half that of a brushless dc system.

The initial requirements used were the maximum power limit of 8 watts, a minimum torque of 2 ounce-inches, and a minimum motor I.D. of 1.0 inch. The parameter used to evaluate the motor design was weight. The initial motor design was not constrained by the overall RWA design so as to provide the opportunity for attaining any advantages of operating speed, form factor, excitation frequency, number of poles, etc. A flow diagram of the motor optimization process is shown on Figure 3-2.

Because of the power limitation of 8 watts, there is a maximum theoretical operating speed limit. This speed is defined by Equation (3-7), which results in a maximum speed (N_R max) of 5408 rpm. In order to evaluate different motor designs, it is useful to consider a measure of an induction motor performance called "stall torque efficiency", ϵ_s, which usually varies over a range of .2 to .8. Stall torque efficiency is defined as

$$\epsilon_s = \frac{P_s}{P_{in}}$$

where

P_s = synchronous load power

$P_{in} = P_s$ + stator losses

ϵ_s is a function of motor weight, impedance and synchronous speed. Choosing a value of $\epsilon_s = .6$, results in a maximum synchronous speed of

$$N_{s_{max}} = .6\ (5408)$$

$$= 3245 \text{ rpm}$$

Note that this is coincidentally the same speed as derived in the paragraph 3.2.1 where the true motor efficiency (η) was used.

In order to provide the required torque over the operating speed range, consideration of the torque-speed characteristic is necessary. Figure 3-3 shows three possible torque speed characteristics which meet the requirement of minimum torque over the operating speed range.

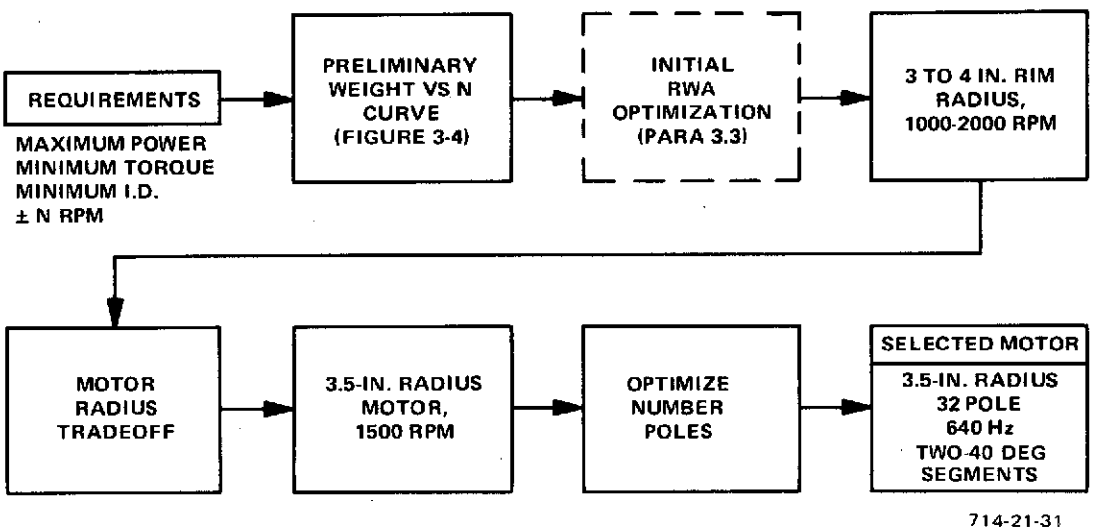

Figure 3-2
Spin Motor Optimization Flow

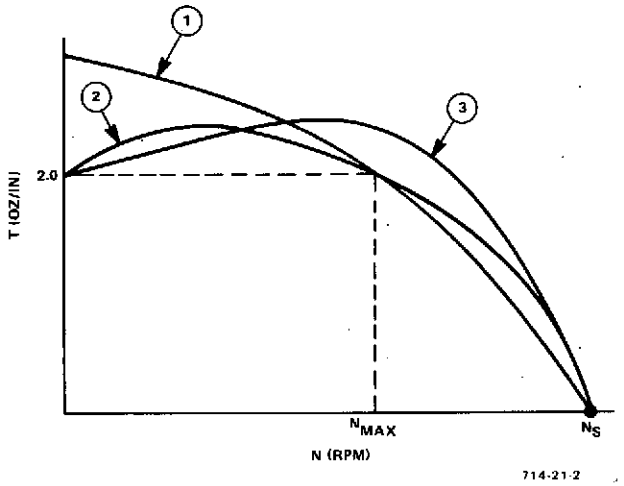

Figure 3-3
Induction Motor Torque/Speed Characteristics

The tradeoff studies showed that characteristic 2 was minimum power at constant weight, and hence was selected as an intermediate design requirement. This aspect of motor design is a function of the ratio of rotor resistance to stator reactance, and can be altered by changing the resistance (material composition) of the conductors in the squirrel cage.

Prior motor design experience has shown that torque-speed linearity is best achieved if the maximum operating speed (N_{max}) is chosen between .5 N_s and .7 N_s. In order to reduce the number of parameters involved in the tradeoff, .6 N_s was chosen as the maximum operating speed. This reduced the RWA operating speed range to $N_{max} < 1950$ rpm for best motor design.

The following motor designs were developed at this point, and illustrate the trend that can be expected.

Motor	ID (in.)	Gap Dia (in.)	Speed (rpm)	Weight (lb)
A	1.0	3.04	1250	.71
B	1.5	3.33	2000	1.75
C	2.125	3.63	2500	2.80

The data is plotted in Figure 3-4, and is used in the RWA optimization (Section 3.3) wherein rotor radius and speed are determined for the minimum weight system.

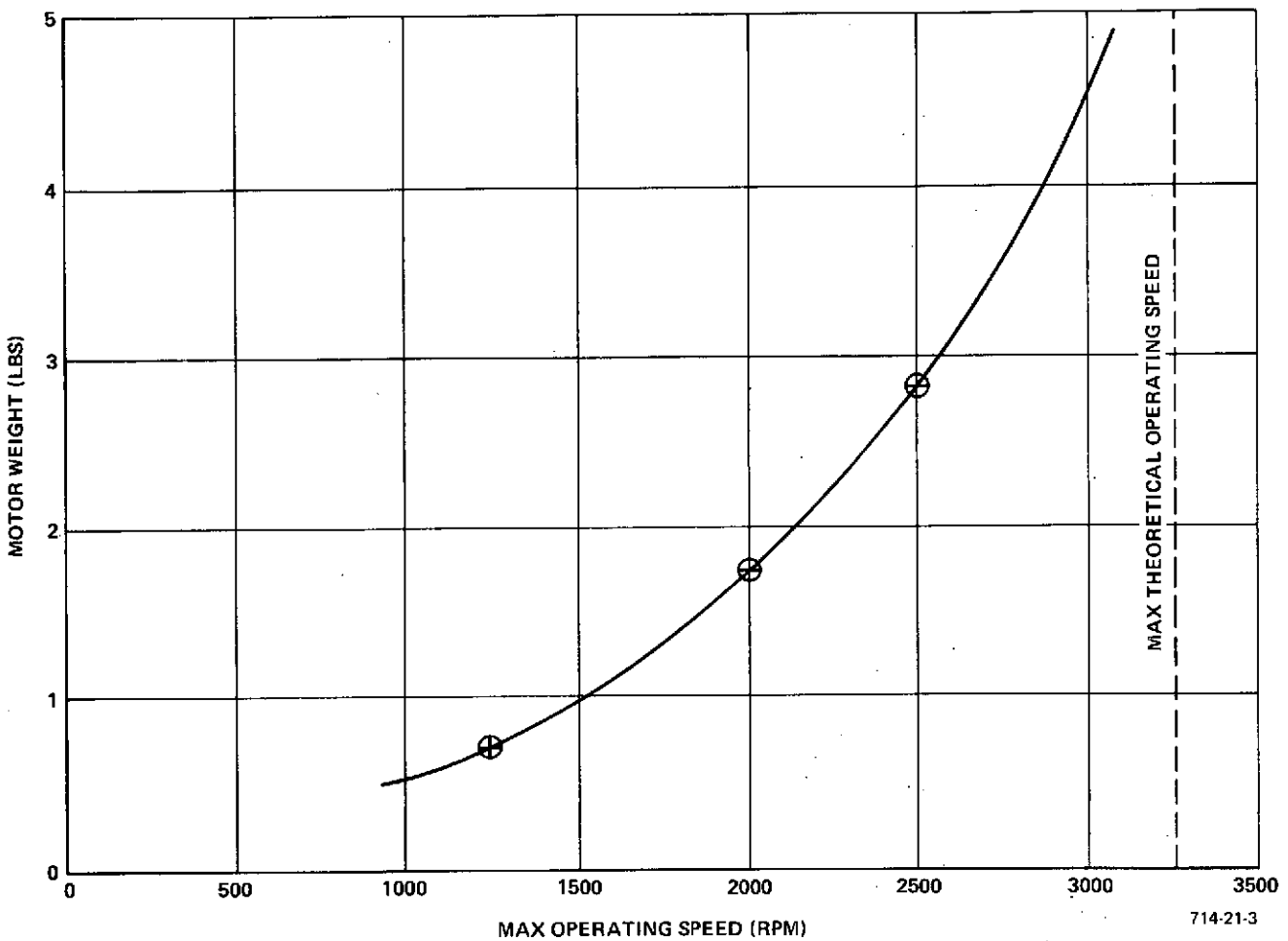

Figure 3-4
Motor Design Optimization Curve

The RWA optimization process in Paragraph 3.3 demonstrated that significant weight savings can be effected by utilization of a large diameter segmented spin motor where the motor cage is also used as the primary inertia element. This fact was incorporated in the motor design calculations, and a speed of 1500 rpm and a radius of 3.5 inches was selected for further optimization. This resulted in the following physical characteristics for the spin motor:

Gap Diameter	7.0 in.
Weight	
Cage	1.0 lb
Stator (2-40° segments)	.6 lb
Poles	32
Excitation	25V, 640 Hz, 2 phase
Maximum Operating Speed (N_{max})	1500 rpm

The performance data (power and torque versus speed) is plotted in Figure 3-5. Note that the minimum output torque is 2.2 ounce-inches and the nominal power is 7 watts; these margins are sufficient to ensure that the requirements of 2 ounce-inches and 8 watts are met in actual production design.

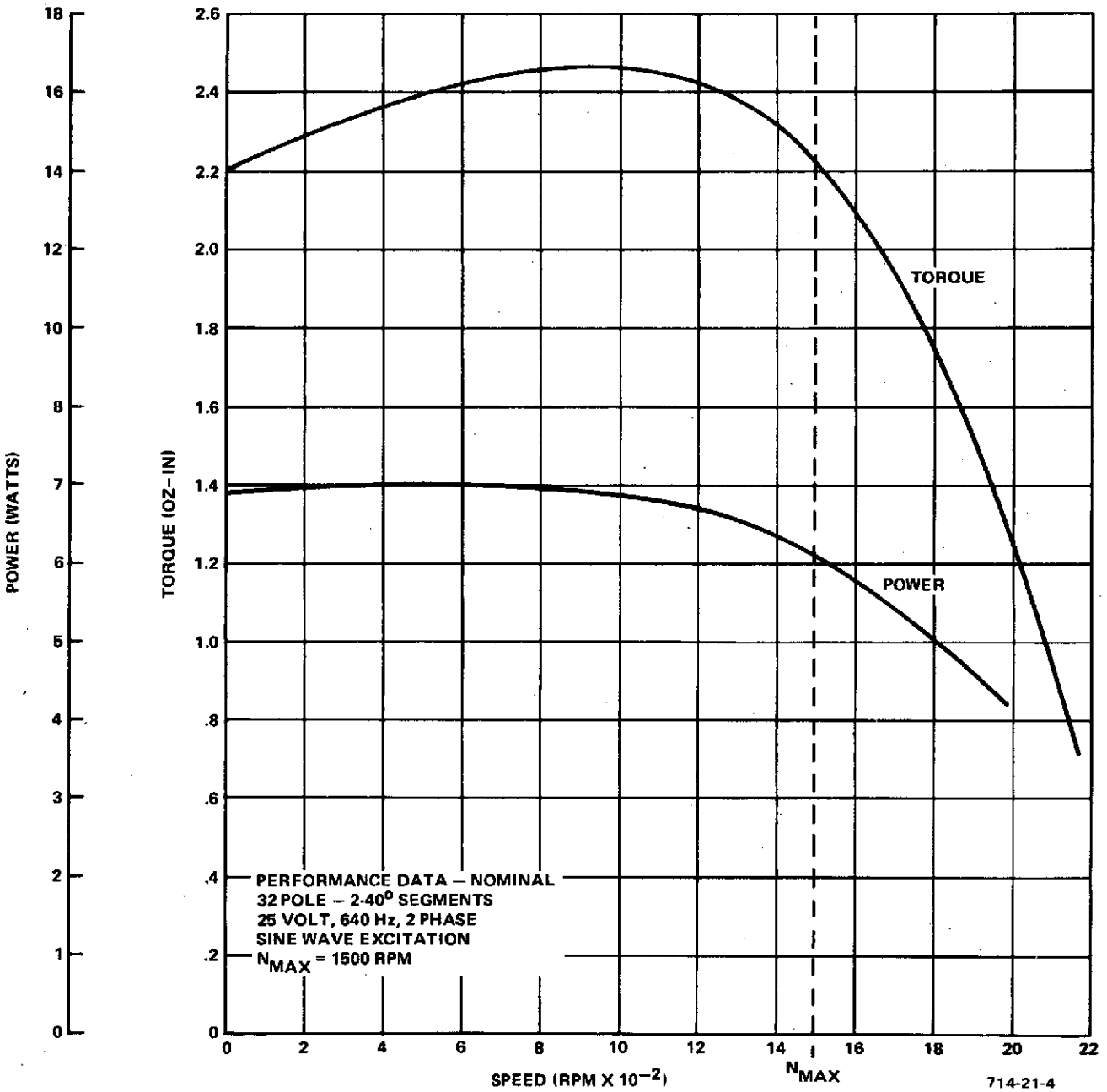

Figure 3-5
Performance Data, Segmented Spin Motor

3.2.3 Magnetic Bearings

The rationale for selection of a dc magnetic, passive-radial, active-axial bearing system was outlined in Paragraph 2.2. Following this, the influences of the actual bearing design on the overall RWA must be examined. The achievement of angular stability dictates the use of two radial-passive bearings with a sufficient axial spacing between them. The stabilizing torque of the bearing pair due to the radial restoring forces then far exceeds the destabilizing torque of each individual bearing due to the axial unbalance forces, thus achieving passive angular stability of the total suspension system. Suitable touchdown means must be designed in order that electronic component failures are safely negotiated before a redundant control system is powered on. Another influence is on the design of the motor, in which the radial clearance must be larger than conventional systems using ball-bearings. In the ac induction motors being considered this increase in radial clearance does not cause a large penalty in motor performance.

In the remainder of this section the constraints on the radial stiffness, the choice of bearing configuration and the design of the bearing are examined.

3.2.3.1 Stiffness Constraints

The design of radial-passive magnetic bearings and their sizing are dependent primarily on the required radial stiffness for the application. The constraints on the radial stiffness based on design considerations/requirements for the reaction wheel are considered separately below.

a. Radial Capacity in a 1-g Environment

It is assumed that touchdown must not occur during operation or test in any attitude, in either a 0-g or a 1-g environment. The most stringent condition is when the wheel is operated with axis horizontal in a 1-g environment, and additional radial deflection due to motor unbalance and under cross-axis rates must be allowed for.

For a magnetic bearing geometry using axially opposed concentric rings a suitable constraint is to limit the allowable deflection under the self-weight to one land width of the concentric ring. Thus

$$K_{r_1} \geq \frac{W_R}{2T} \text{ (lb/in.)} \qquad (3\text{-}9)$$

where

K_{r_1} = required radial stiffness per bearing

W_R = total suspended rotor weight (lb)

T = width of a ring land (in.)

To ensure that the unbalance stiffness ratio is a minimum, the smallest possible T must be chosen; the minimum value consistent with manufacturability is T ≈ .014 inch. The minimum radial stiffness is thus a linear function of the rotor weight and the variation is plotted in Figure 3-5.

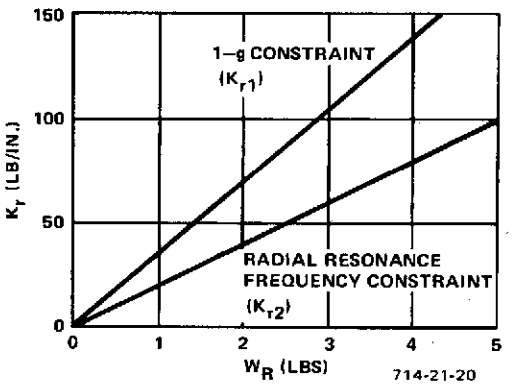

Figure 3-6
Minimum Radial Stiffness due to 1g Capacity and
Radial Resonance Frequency

b. Radial Resonant Frequency

Considering the rotor as a rigid body, the radial resonant frequency (f_r) is

$$f_r = \frac{1}{2\pi}\sqrt{\frac{2K_{r2}\, g}{W_R}} \quad \text{(Hz)} \tag{3-10}$$

If a minimum f_r is specified, the constraint on stiffness simplifies to

$$K_{r_2} \geq \frac{\pi^2 f_r^2 W_R}{6g} \quad \text{(lb/in.)} \tag{3-11}$$

where

K_{r_2} = required radial stiffness per bearing

W_R = rotor weight (lb)

$g = 32.2$ ft/sec^2

Since it is desired to maintain wheel resonances above 20 Hz to avoid interactions with the spacecraft,

$$K_{r_2} \geq 20.45\, W_R \tag{3-12}$$

which is a linear function, and is also plotted in Figure 3-5. It may be noted that the 1g constraint on stiffness is more severe than that based on the radial resonance frequency.

c. Angular Resonance Frequency

If the angular stiffness (K_α) is assumed to be due purely to the radial restoring forces in each bearing, then

$$K_\alpha = 1/2\, K_r\, \ell^2 \text{ (in.-lb/radian)} \tag{3-13}$$

where

K_r = radial stiffness per bearing (lb/in.)

ℓ = axial bearing span (in.)

In practice, however, the restoring torque due to the radial forces is diminished by torques due to the axial unbalance forces. (The exact expression for the angular stiffness is obtainable only as a derivative of the total co-energy of the system w.r.t. the angular displacement.) On the basis of laboratory measurements, a conservative value for preliminary design is

$$K_\alpha = 1/4\ K_r\ \ell^2 \tag{3-14}$$

The angular resonance frequency for the RWA is a function of wheel speed because of the gyroscopic interactions; however, the minimum resonance frequency (f_α) corresponds to the nonrotating condition and is given by

$$f_\alpha = \frac{1}{2\pi}\sqrt{\frac{K_\alpha}{I_t}}\ \text{(Hz)} \tag{3-15}$$

where

K_α = the angular stiffness (in.-lb/rad)

I_t = the transverse inertia of the rotor (in.-lb-sec^2)

Solving Equation (3-14) and using a specified minimum of f_α,

$$K_\alpha \geqslant 4\pi^2\ f_\alpha^{\,2}\ I_t \tag{3-16}$$

The rotor polar inertia (I_R) is typically 60 percent of the transverse inertia (I_t). Combining this relationship with Equation (3-6) and substituting into Equation (3-15) yields the following constraint: (H = .5 ft-lb-sec).

$$K_{r_3} \geqslant 58.92\ W_R \left(\frac{R}{\ell}\right)^2\ \text{lb/in.} \tag{3-17}$$

where

K_{r_3} = required radial stiffness per bearing

W_R = rotor weight (lb)

R = rotor radius (in.)

ℓ = axial bearing span (in.)

This equation is plotted in Figure 3-7 as a function of the rotor weight (W_R) and the ratio R/ℓ for expected values in the RWA.

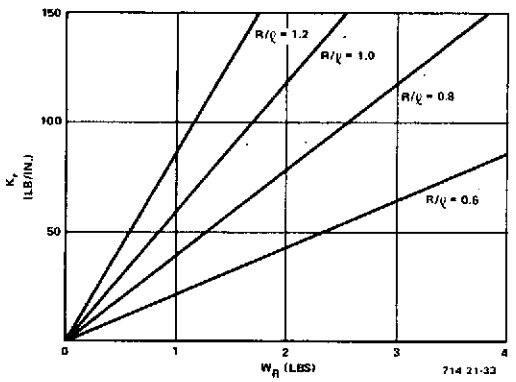

Figure 3-7
Minimum Radial Stiffness due to Angular Resonance Frequency

d. Cross-axis Rate

Under a cross-axis rate Ω, the angular deflection (α) is given by

$$\alpha = \frac{12\ \Omega\ H}{K_\alpha} \text{ (radians)} \qquad (3\text{-}18)$$

where

K_α = the angular stiffnes (in -lb/radian)

H = the angular momentum (ft-lb-sec)

The angular deflection is related to the radial deflection (δ) at each bearing by

$$\alpha = \frac{2\ \delta}{\ell} \qquad (3\text{-}19)$$

where ℓ is the axial bearing span. Substituting for K_α in terms of K_r gives the constraint

$$K_{r_4} \geqslant \frac{24\ \Omega\ H}{\ell\delta} \qquad (3\text{-}20)$$

For H = .5 ft-lb-sec, and the specified value of Ω = 17.5 mr/sec,

$$K_{r_4} \geq \frac{.21}{\ell\delta} \text{ lb/in.}$$

where ℓ and δ are in inches.

Thus, if we consider ℓ = 3 inches and δ = .001 inch as minimum values, this constraint gives

$$K_{r_4} \geq 70 \text{ lb/in.} \qquad (3\text{-}21)$$

The above four constraints [Equations (3-9), (3-12), (3-17), (3-20)] considered determine a minimum value of radial stiffness of the magnetic bearing. Examination shows that for $R/\ell \geq .6$ the constraint due to angular resonance frequency dominates those due to the 1-g radial capacity and the radial resonance frequency. In addition, if $R/\ell > 1$, the constraint also dominates that due to maximum cross-axis rate for $W_R \geq 1.2$ pounds. For the representative value R/ℓ = 1.0, the required radial stiffness ranges from 70 pound/inch for a rotor weight of 1 pound, to 167 pound/inch for a rotor weight of 3 pounds. Selection of the final value of K_r is made in paragraph 3.2.3.3.

It may be noted that no restriction has been placed on the location of the resonance speeds relative to the range of operating speeds for the RWA. Thus, it is possible that a radial or angular resonance speed may be traversed during wheel operation. This decision was based on tests on the Sperry magnetic bearing model where it was determined that resonance speeds could be dwelt on for extended periods without significant increases in motor or bearing power; the radial excursions were also well-bounded. If the resonance speeds were constrained to be above the operating range, this would entail an unduly large bearing radial stiffness with an attendant penalty in bearing weight.

3.2.3.2 Bearing Configuration

For implementing the radial-passive, axial-active, attraction concept selected, the three-loop bearing configuration was used as a starting point. (This configuration has been used for the Sperry magnetic bearing model as well as for the suspension of a large 700 ft-lb-sec momentum wheel assembly.) Following this, the one-loop bearing was examined as an alternative for the small RWA application. This bearing concept, also previously developed, has the advantage of simplicity. Both configurations are described below.

a. Three-Loop Bearing

A schematic of the configuration is shown in Figure 3-8. It is termed a three-loop bearing because three independent loop equations are required to analyze the magnetic circuit.

The bias magnetic flux (B_o) is provided by the axially magnetized ring magnets across four axial gaps, the direction of the bias flux being shown by the arrows in the figure. The passive radial stiffness is provided through the action (minimum reluctance) of opposed concentric rings at the air gaps, the total stiffness being proportional to the number of rings. Radial damping is provided with conducting material, e.g., copper wire, placed between the rings at the air gaps.

In the axial direction, the bias fields cause instability. Axial control forces are provided by modulating the gap bias fluxes; this is accomplished by varying the magnitude and direction of the current to the two control coils in response to a position error signal. Thus, the coils are connected such that the bias flux is increased in one pair of gaps by an amount ΔB while it is decreased in the other pair of gaps; the result is an axial force proportional to $8B_o \Delta B$, as shown in Figure 3-9.

The significant features of the three-loop configuration can be summarized as follows:

- Both magnets and coils are stationary
- The coil currents must overcome only the air-gap reluctance
- The axial stiffness obtainable is proportional to the bias field, which permits higher gains at lower power levels
- Radial damping is provided by copper rings
- Pole pieces are used to minimize flux variations at the gaps

b. One-Loop Bearing

The terminology "one loop" here again refers to the fact that both the permanent magnet and control coil establish flux in the same magnetic circuit loop, and the determination of this single loop flux is sufficient for a magnetic circuit analysis. The one-loop bearing is shown in Figure 3-10.

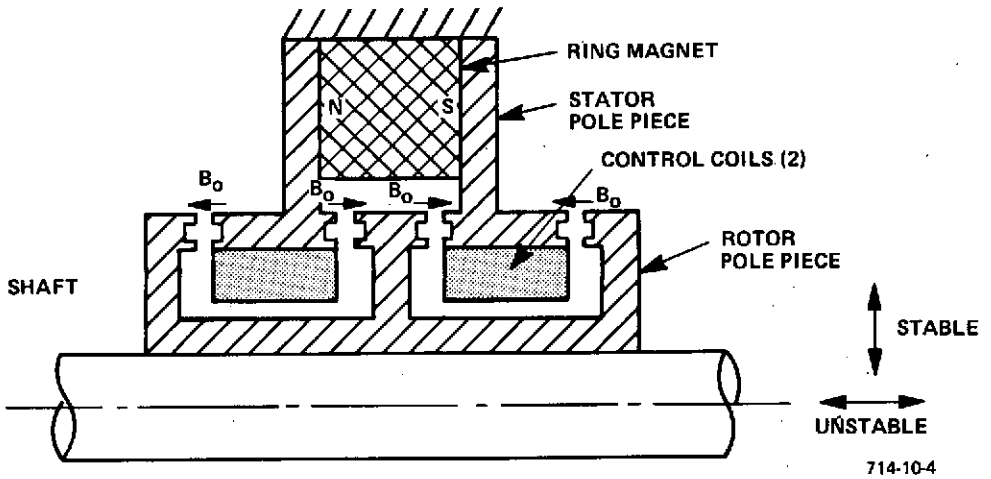

Figure 3-8
Three-Loop Bearing, Half Section

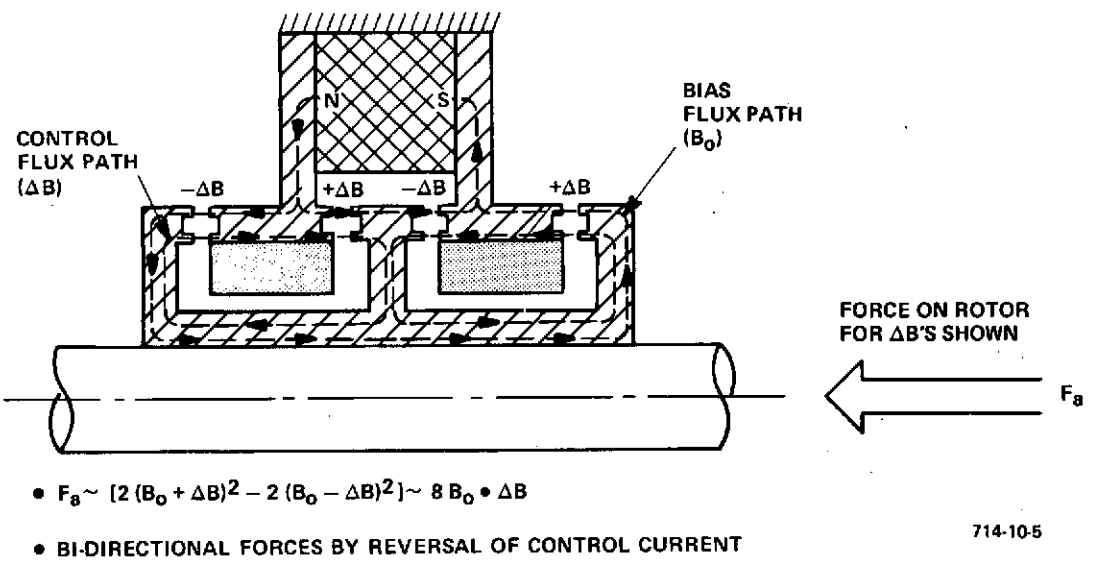

Figure 3-9
Axial Control Force Generation

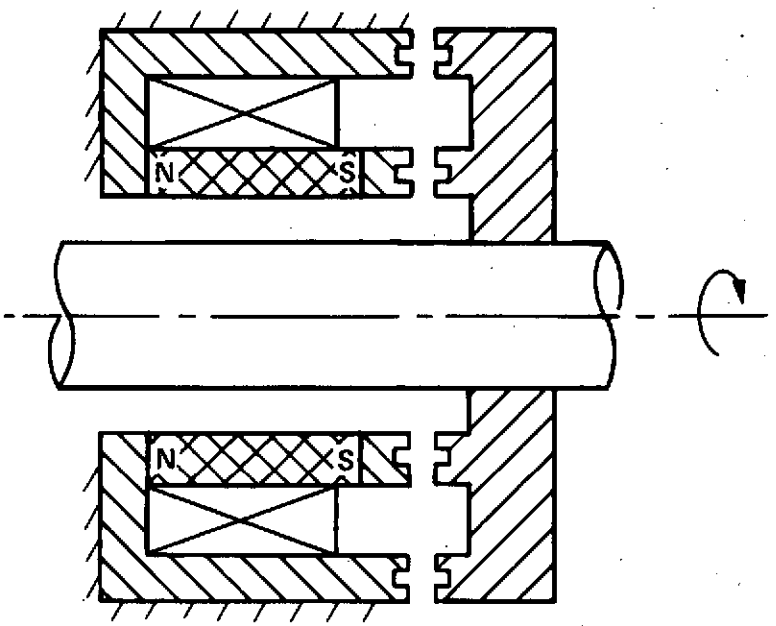

714-21-22

Figure 3-10
One-Loop Bearing Configuration

The bias flux is again provided by the permanent magnet, and passive radial stiffness is attained through the action (minimum reluctance) of opposed concentric rings. Bidirectional axial control forces are provided by modulation of the gap flux by controlling the current in the coil.

The primary disadvantage of the one-loop configuration compared to the three-loop configuration is that the control current must counter the reluctance of the permanent magnet in the one-loop design. This means that larger control currents are necessary to produce the same axial force, entailing larger power loss under dynamic loads. In addition, high-coercivity permanent magnet materials such as rare-earth cobalts are essential to prevent the possibility of demagnetization. Analysis shows that the reduction in the force-to-current gain because of the extra magnet reluctance is only 50 percent for the case where the circuit is designed for minimum magnet volume, and can be lower at the cost of some additional penalty in magnet volume.

Since the passive radial stiffness is proportional to the square of the flux density, it is desirable to provide as high a bias flux density as possible, allowing for sufficient margin for modulation before saturation. Considering that the flux density at saturation for soft material such as electromagnet iron is in the range of 1.6 to 2.0 Wb/m^2, a bias density level of 1.4 Wb/m^2 is a suitable value for design; this leaves an adequate margin for modulation to develop axial control forces.

Sizing a three-loop bearing for this bias flux density shows that for a mean radius of .6 inch at the rings, and for merely 1 ring/gap, the radial stiffness per bearing is

$$225 \text{ lb/in.} \leqslant K_r \leqslant 554 \text{ lb/in.}$$

where the upper limit is based on an infinite-width geometry stiffness analysis and the lower limit on a line-potential geometry. Comparison with the required radial stiffness for expected rotor weights (70 lb/in. to 167 lb/in.) shows that the minimum radial stiffness in a three-loop bearing exceeds the requirements. The weight of such a three-loop bearing pair, including magnets, coils, and pole pieces is estimated at 1.6 pounds.

Following this, a one-loop bearing was sized, for $B_g = 1.4$ Wb/m^2, and a radius to the outer rings of .6 inch. The stiffness K_r was bounded in the range

$$167 \text{ lb/in.} \leqslant K_r \leqslant 410 \text{ lb/in.}$$

The weight of this bearing pair is estimated at .6 pound. The weight comparison, the design simplicity, the fewer number of machined parts and ease of manufacture and assembly were the basis for the selection of the one-loop design for this RWA application. For the initial weight trade-off, the weight of the shaft and stator support hardware was added to the actual bearing weight, and for the expected stiffness range this total weight of the magnetic bearing system (W_{MB}) is:

$$W_{MB} = .4\ W_R \quad \text{(lb)} \tag{3-22}$$

3.2.3.3 Design of the One-Loop Bearing

Following the selection of the one-loop bearing configuration for the RWA, the next step is the design of the magnetic circuit. Designing the magnetic circuit involves the design of the gap geometries and magnetic structures, choice of magnetic materials, and sizing of the permanent magnet and the control coil. An important design parameter to be established at this point is the unbalance stiffness ratio. This is the ratio of the axial unbalance stiffness to radial stiffness for the passive magnetics and is the main parameter coupling the radial and axial axes.

a. Radial System

The preliminary analyses on RWA sizing indicate that the total rotor weight is likely to be in the range of 2 to 3 pounds. The design value for radial stiffness is therefore taken as 167 pounds/inch, corresponding to the 3 pound rotor weight. For the one-loop bearing, the initial radial stiffness is given by

$$K_r\big|_{r\,=\,0} = \alpha\ (n_1\ r_1 + n_2\ r_2)\ B_g^{\,2} \tag{3-23}$$

where

α = coefficient dependent on geometry

n_1 = number of rings at radius r_1

n_2 = number of rings at radius r_2

and

B_g = the peak flux density in the gap.

In order that the axial spacing between bearings is not excessive, a value r_1 = .6 inch is taken as a constraint. For B_g = 1.4 Wb/m^2, the remaining values for a ring width T = .014 inch work out to be n_1 = 2, r_1 = .3 in., r_2 = 2.

The magnet material chosen for the design is samarium-cobalt, because of

- Its high energy-product, allowing a decrease in weight over Alnico
- Its reversible, straight-line demagnetization characteristic and high intrinsic coercive force. This is especially important in the one-loop bearing design, because the control flux, which passes through the magnet, will oppose the permanent magnet flux when it is desired to decrease the flux density in the gap. The B-H characteristic also enables the magnet to be magnetized prior to assembly and eliminates the need for keepers.

Sizing the magnet for a nominal axial gap of .015 inch and B_g = 1.4 Wb/m^2 gives

$$A_m = 1.3 \text{ in.}^2, \ell_m = .120 \text{ in.}$$

where A_m is the cross-sectional area of magnet and ℓ_m is the axial length. The magnet is designed to operate at its $(BH)_{max}$ point, to give minimum volume of magnet material.

b. Axial System

The objectives here are to determine the expected axial unbalance stiffness, the net axial stiffness under feedback and the required coil ampere turns.

For the chosen geometry, the unbalance stiffness ratio is estimated as

$$\frac{K_u}{K_r} = -8 \qquad (3\text{-}24)$$

The total axial unbalance stiffness (for both bearings) that must be overcome by the axial control system is

$$K_u = -2 \times 8 \times 167 = -2672 \text{ lb/in.}$$

Under position-rate feedback, with the requirement that lift-off and control be possible from a single coil (i.e., allowing for the provision of redundancy), the feedback position gain for stability is

$$K_\psi = 35.9 \text{ AT/M} = 91{,}000 \text{ AT/in.}$$

Considering a maximum axial travel before touchdown of .008 inch, the required coil capacity for lift-off is 8 x 91 = 728 AT. The achievement of net axial stiffness means that some margin must be provided above this. A value of 1100 AT is chosen. Having determined the basic parameters for the design, the pole pieces (to be made from electromagnet iron) and the control coils are sized suitably to complete the design. In order to prevent clamping and reaction forces being applied to the magnets, a non-magnetic spacer is used to separate the stator pole pieces.

3.2.4 Suspension Control System

The suspension electronics provides the axial control forces to maintain levitation of the rotor. The main components, as shown in Figure 3-11, are the axial position sensor, compensation network, power amplifier, and an integrator. Power consumption is minimized by the integrator, which causes the system to operate at zero steady-state coil current. The primary design considerations are maximum reliability and minimum power consumption.

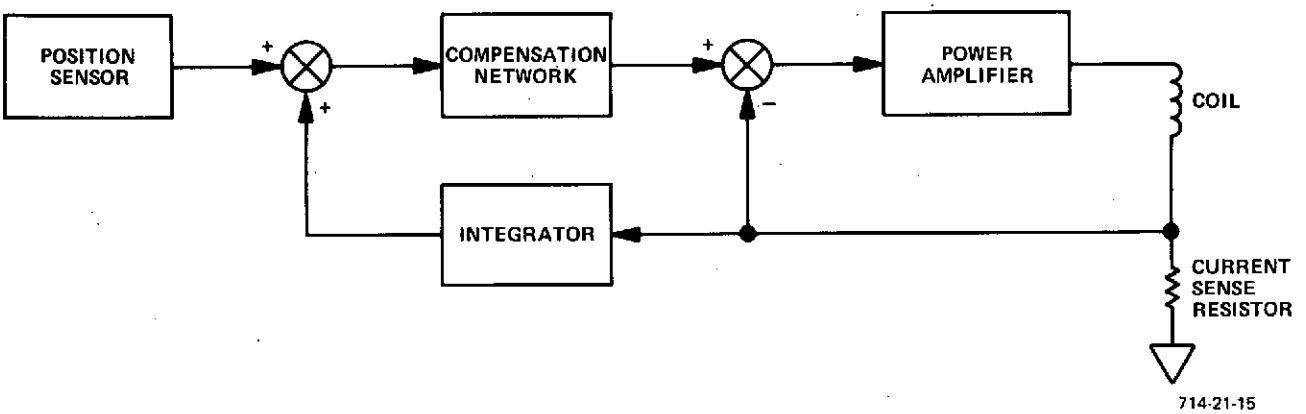

Figure 3-11
Suspension Electronics Block Diagram

3.2.4.1 Position Sensors

Various types of noncontacting position sensor are capable of measuring distances on the order of .005 to .035 inch, as required in this application. Of these, the two offering the most advantages are the capacitive transducer and the eddy current transducer.

The capacitive transducer, Figures 3-12 and 3-13, contains an ac source and two capacitors which are the two parts of a differential capacitor. The capacitor plates are discs. The center plate is fastened to the rotor shaft, and the two outside discs are mounted on the frame but are electrically insulated from it. For an axial displacement to the left in Figure 3-12, capacitor C1 will increase and C2 will decrease in capacitance. This change is detected by the sensor electronics and results in an error signal output to the suspension electronics.

Since the rotor is suspended magnetically, there can be no physical electrical connection to the shaft. The electrical circuit is completed by means of capacitor C_s between the shaft and ground. This consists of the capacitance between the rotor and the fixed elements of the wheel, i.e., the housing, the center tie bar, etc. This capacitor must be large compared to the elements of the differential capacitor.

The capacitive transducer is simple, has good linearity and is insensitive to temperature variations and variations of the source frequency. For a plate area of .5 square inch, a sensitivity of .140 volt per mil of displacement is achievable.

In the eddy current sensor (Figures 3-14 and 3-15) an ac source excites a probe which is simply a small coil of wire oriented so that the induced field intersects the sensed surface. The surface must be a conductor so that eddy currents are induced into it. The closer the probe to the sensed surface, the greater the eddy currents will be.

The electronic circuit converts the eddy current variations into a dc signal. The ac oscillator excites the probe through a high source impedance. The voltage across the probe then varies as the coil impedance changes. The voltage is converted to dc by rectification and filtering.

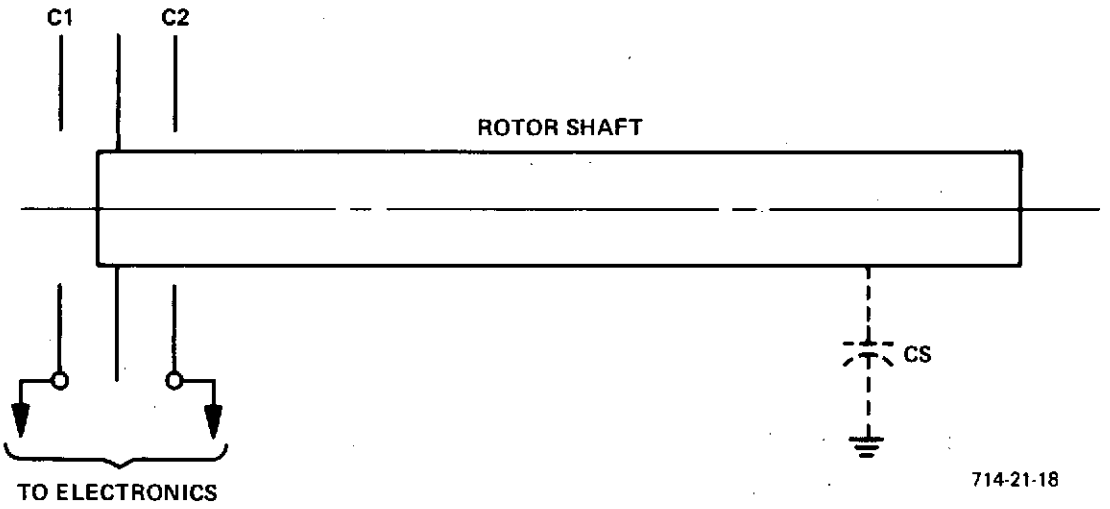

Figure 3-12
Differential Capacitor

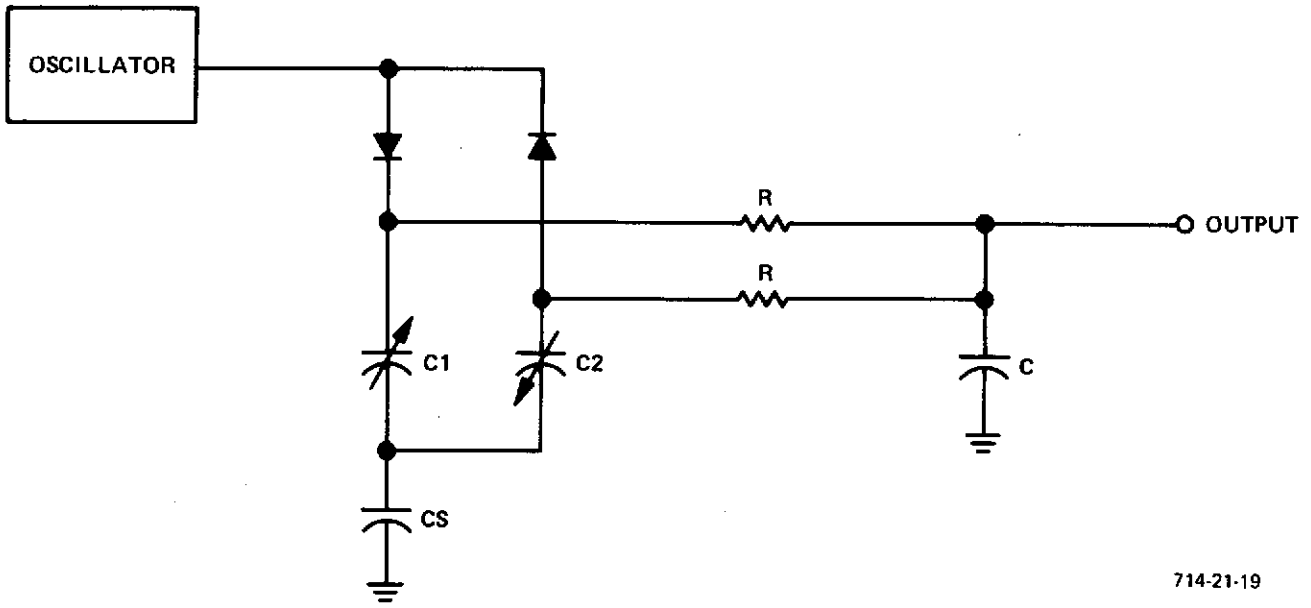

Figure 3-13
Capacitive Transducer Circuit

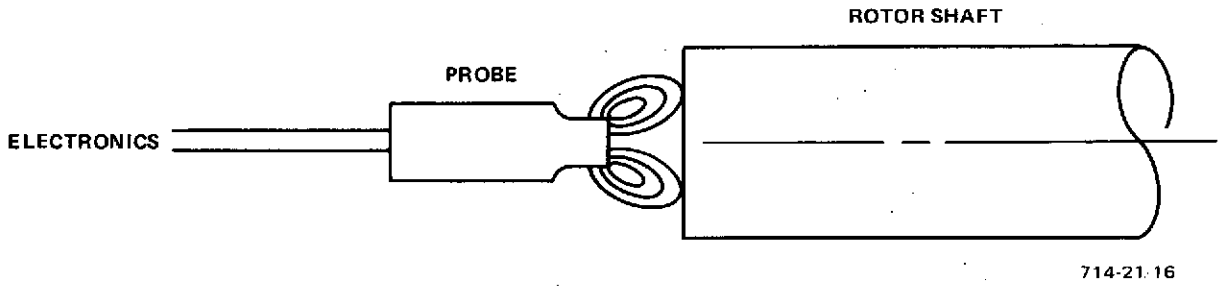

Figure 3-14
Eddy Current Sensor

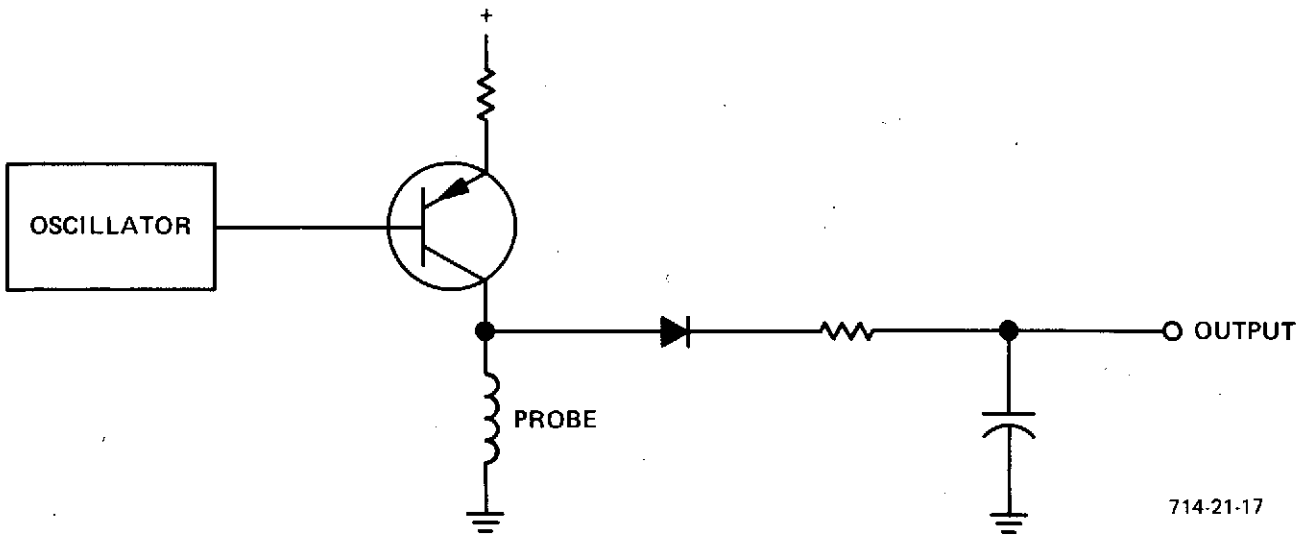

Figure 3-15
Eddy Current Transducer Circuit

The eddy current sensor can provide an output scale factor of .3 volt per mil and has good linearity. It is somewhat sensitive to temperature and excitation frequency changes, but in the magnetic bearing application this is not critical.

In choosing between the capacitive transducer and the eddy current sensor, the main consideration is mechanical, i.e., the mounting of the probe versus the plates or rings in the wheel assembly. The probe of the eddy current sensor should be mounted directly at the center of the end of the shaft to minimize pickup of angular motions and mechanical runout. Otherwise signals at the rotational frequency will be input to the suspension electronics, resulting in additional steady state power. The capacitive sensor with rings around the shaft will average out any rotational frequency inputs.

The eddy current sensor was chosen for the RWA because of the less complicated mechanical interface - while the capacitive sensor has some advantages, they were not sufficient to warrant its use in a small wheel of this nature.

3.2.4.2 Power Amplifier

The power amplifier consists of a bridge which controls currents in either direction through the coils in response to signals from the position sensor. The compensation in the form of a lead/lag network, is included as a part of the amplifier. Figure 3-16 is a schematic of the amplifier showing the use of several operational amplifiers. The availability of new microcircuits containing four, very low-power operational amplifiers on a single chip makes it advantageous to replace discrete circuits with these devices. One small penalty associated with the use of operational amplifiers is that it is necessary to generate plus and minus power voltages from the +28 volt dc input power. The use of ±8 volts used with 5 volt signals is selected over the more common ±15 volts and 10 volt signals to conserve power. Each operational amplifier will use less than 5 milliwatts of power. The net savings of number of components and power consumption justifies this approach.

The maximum permissible power consumption of the suspension system is 1 watt. This is achieved with considerable margin as seen in the next paragraph. The maximum power consumption at lift-off is 8 watts. This is accomplished by designing the coils to have a relatively high resistance by using many turns of small wire which limits the amount of power that can be drawn from the +28 volt

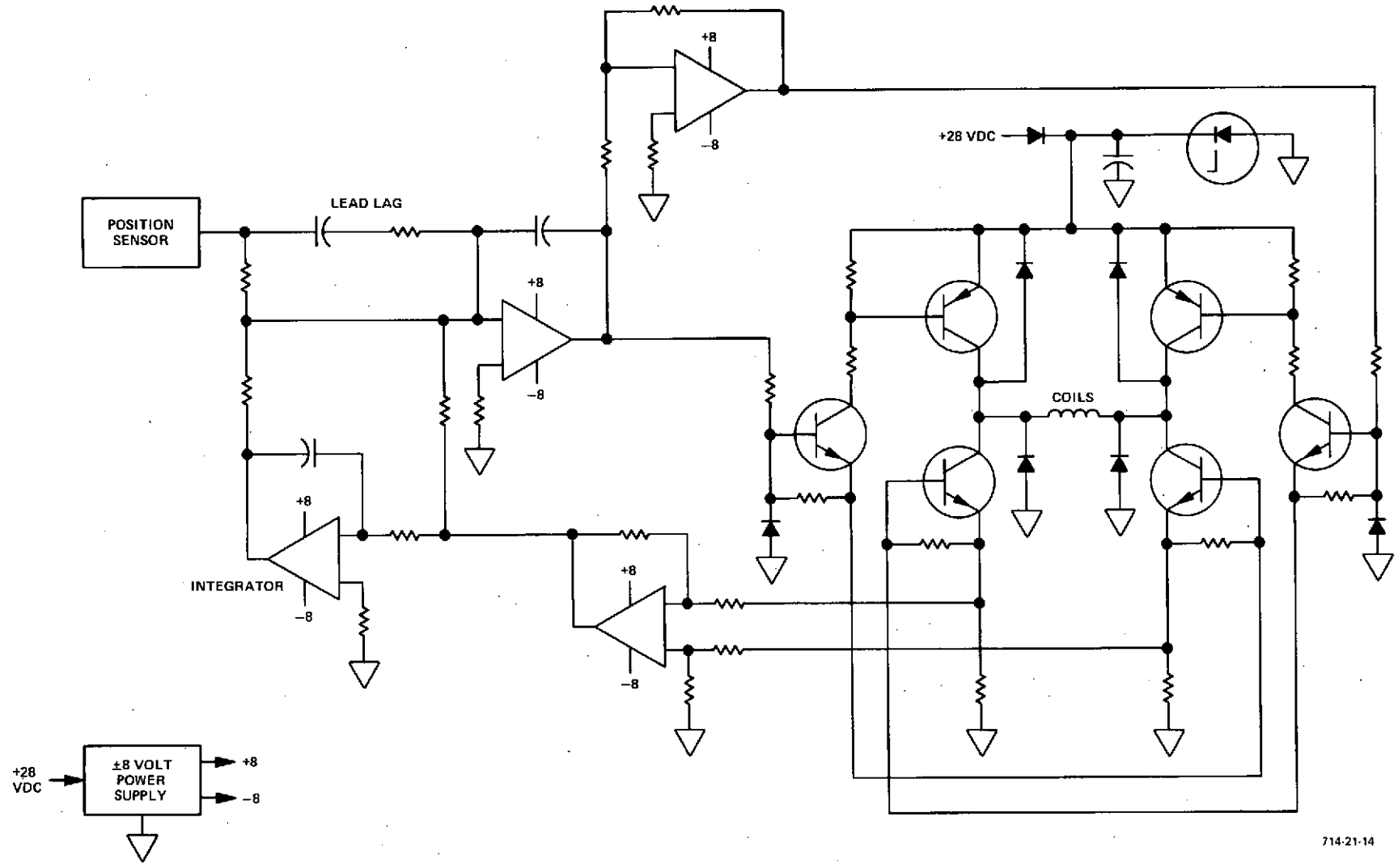

Figure 3-16
Power Amplifier Schematic

line when the amplifier is turned on. The force capacity of the coils is reduced this way, but it is possible to maintain adequate capacity and still reduce the total power to under 8 watts.

3.2.4.3 Power Breakdown

The calculated power consumption of the suspension electronics is given in Table 3-2. This assumes that the wheel speed is not at any of the resonances and that the position sensor is situated so that very little rotational motion is detected. The position sensor contains an oscillator operating at 1 megahertz. In the power amplifier, the bridge uses some power because it is impossible to eliminate all rotary motion effects and other disturbances from the input. The power supply provides ±8 volts for the position sensor and the operational amplifiers, and it operates with an efficiency of about 50 percent.

TABLE 3-2

CONTROL ELECTRONICS POWER CONSUMPTION

Component	Power (mw)
Position Sensor	96
Power Amplifier	
Operational Amplifiers	20
Bridge	140
Power Supply	116
Total	372

3.2.4.4 Reliability

The failure rate of the suspension electronics is estimated to be less than one failure per million hours. The breakdown is as shown in Table 3-3.

TABLE 3-3

ELECTRONICS RELIABILITY

Component	Quantity	Total Failures per 10^6 hr
Sensor	1	.050
Power Bridge	26	.196
Op Amps	4	.510
Power Supply	10	.104
	41	.860

3.2.5 RWA Housing

The housing for the magnetic suspension reaction wheel assembly is basically a cylinder whose radius varies with rotor radius and whose height is relatively constant. The height is determined primarily by the magnetic suspension system which requires a length/diameter ratio = 3.0 with a minimum diameter of 1.0 inch. The mounting of the axial proximeter adds .6 inch to the overall height, resulting in a basic configuration as shown in Figure 3-17. The weight of the housing is the sum of the weights of the five basic parts as shown. All material in the housing is aluminum.

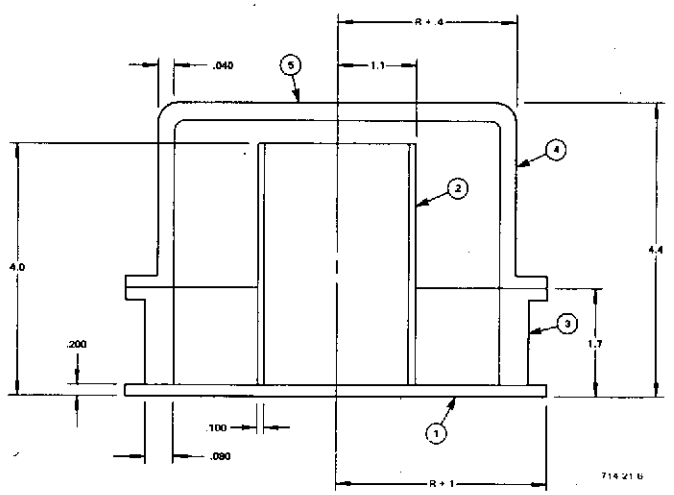

Figure 3-17
RWA Housing Weight Model

The weight of the housing is shown in the table below for $1 \leq R \leq 5$ (R = Rotor radius) in terms of each element, and is plotted on Figure 3-18.

Rotor Radius	Element					
	1	2	3	4	5	Total (lb)
1	.188	.264	.108	.093	.025	.678
2	.565	.264	.203	.161	.072	1.265
3	1.01	.264	.288	.299	.148	1.939
4	1.57	.264	.374	.297	.247	2.752
5	2.26	.264	.460	.364	.372	3.720

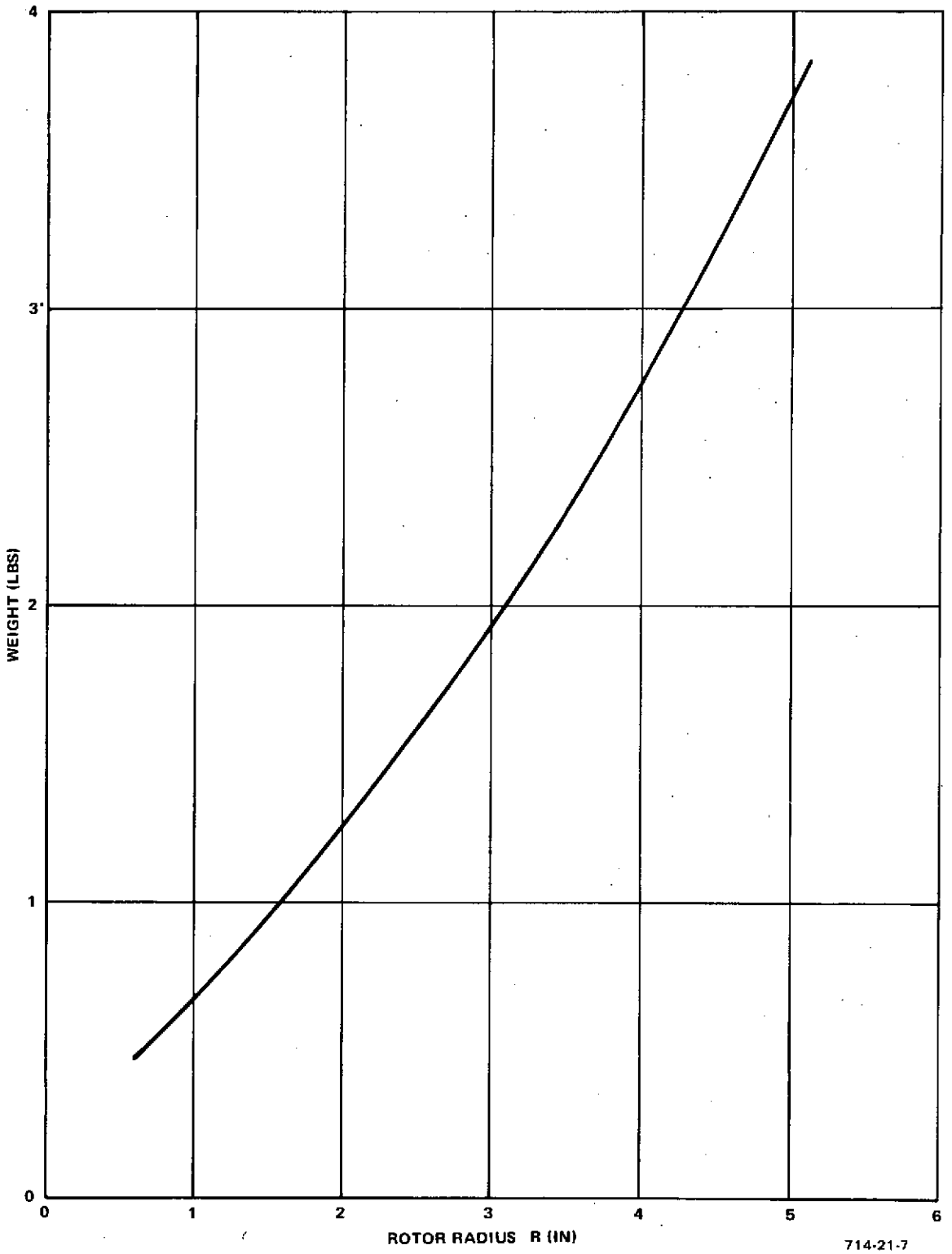

Figure 3-18
Housing Weight Versus Rotor Radius

3.2.6 Touchdown System

The touchdown system of a magnetically suspended RWA provides protection for the magnetic pole pieces during launch, and also in the event of electronic failureor turn-off of the suspension electronics during operation. The clearances in the touchdown bearings are less than the clearances between the pole pieces, thereby preventing their physical contact. The touchdown system also prevents contact of the spin motor rotor and stator in the radial direction.

The touchdown system must be capable of absorbing the impact of touchdown, and also capable of dissipating the energy in the wheel at maximum speed. One approach is to use ball bearings, with a large clearance between the rotating element and one bearing race. A second approach is to use a journal thrust bearing instead of the ball bearing. This second approach has the advantages of not requiring a lubricant, and is adaptable to most concepts without compromising the full utilization of the available space by the magnetic suspension.

The use of journal bearings was chosen for the reaction wheel design. A survey of potential materials was made and a Garlock product, DU, was chosen for this application. DU is a prefinished high performance bearing material that requires no lubricant, is an inert material, and presents no outgassing problem. The material is made up of three bonded layers: 1) a backing strip of steel, 2) a middle layer of porous bronze, the bores being solidly filled with TFE (polytetraflouroethylene) and lead, and 3) a surface layer (.001 of the same TFE-lead mixture.

The life of a DU bearing is a function of the load pressure and the velocity of rotation. In this application the load pressure in the axial direction is

$$\frac{Fu}{A_B} = \frac{25 \text{ lb}}{.26 \text{ in.}^2} = 96 \text{ lb/in.}^2$$

and the maximum velocity is

$$V = N \times \frac{\pi d}{12}$$

$$= 1500 \times \frac{\pi (.7)}{12}$$

$$V = 275 \text{ ft/min}$$

The product PV = (275)(96)

$$= 26400$$

The life (H) at this load rating for a thrust bearing, which is the load situation for a touchdown is

$$PV = \frac{12 \times 10^6}{H + 200}$$

$$H = \frac{12 \times 10^6}{PV} - 200$$

$$= \frac{12 \times 10^6}{26400} - 200$$

$$= 455 - 200$$

$$H = 255 \text{ hrs}$$

Since this application is one that is encountered only in test and for a failure mode during operation, the life is adequate.

The coefficient of friction for these conditions (< 500 psi, $10 \leqslant V \leqslant 1000$ fpm) is 0.1-0.2, which produces a torque of

$$T = .2\ (25)\ (.35)$$

$$= 1.75 \text{ in. lb}$$

$$T = 28 \text{ oz in.}$$

The energy in the reaction wheel at maximum speed (1500 rpm) is

$$E = 1/2\ H\omega$$

$$= 1/2\ (.5)(1500)\left(\frac{2\pi}{60}\right)$$

$$E = 39.3 \text{ ft lb}$$

$$= .0506 \text{ BTU}$$

The bearing material has a specific heat of .2 BTU/lb °F, and weighs .004 pound. The temperature rise during a touchdown from 1500 rpm is 63°F which is well within the operating limit of the material.

The load rating of DU for fluctuating loads at less than 10^5 cycles is 4000 psi, which provides adequate margin for the conditions encountered in a touchdown situation.

The shock and vibration capability of a ball bearing reaction wheel is usually limited by the load carrying capacity of the bearings. The ball bearings are stiff, resulting in relatively high natural frequencies, which are associated with the higher energy inputs. The bearings must not be brinelled by these loads in order to rpvode smooth operation on orbit.

The magnetically suspended reaction wheel, however, is designed such that these launch loads are taken by the touchdown system, which is not in contact during operation, and hence must only survive without deformations of more than .003-.005 inch. The contact surface in a journal type touchdown system is significantly larger than that of a ball bearing, which is another factor in the shock and vibration capability of the design. The effect of the nonlinear nature of the clearance in the touchdown system has not been evaluated, but should also be a plus feature because of its inherent damping.

It is expected that the magnetically suspended reaction wheel will not encounter any significant problems due to shock or vibration loads.

3.3 RWA DESIGN CONCEPTS

The three primary elements in a reaction wheel optimization are:

- Rotor
- Housing
- Spin Motor

The peak power requirement of this study places an upper limit on maximum operating speed, but does not limit the optimization process, as will be seen later. The three primary components used in the tradeoff can take many different characteristics depending on the general configuration desired. For example, the spin motor length/diameter ratio can vary from a typical servo motor shape to a pancake configuration. The housing can vary from a cg mount to an end mount, and can be round or square. The rotor web can be spoked, flat, conical, or umbrella and when combined with a large diameter motor cage, could require little or no rim. The large OD pancake type motor lends itself very nicely to the concept of a redundant motor stator, since the torque capability increases rapidly with diameter, usually requiring only a portion of the 360 degrees available for the stator.

Two possible concepts are shown on Figures 3-19 and 3-20 as examples of the extremes that the RWA configuration can take. The general shape of the magnetic suspension elements can also affect the optimization process. If these elements are mounted in a manner similar to that shown in Figures 3-19 and 3-20, the result is a longer axial dimension, and hence increased housing weight. The most weight effective design approach results in a dense package with the inertia element at as large a radius as possible. This philosophy resulted in the concept shown in Figure 3-21. The fact that the touchdown system is embodied in the covers and the irregular mounting base configuration were not among the most deairable features. These were corrected in the concept of Figure 3-22. It was this basic configuration that was used in the optimization process.

The basic component weight curves are shown in Figures 3-1, 3-4 and 3-18. Combining this data, and approximating the magnetic suspension weight as .4 times the rotor weight [Equation (3-22)] results in the RWA weight curves shown in alternate forms in Figures 3-23 and 3-24. This optimization indicates that a wheel of 3 to 4 inches radius at 1000 to 2000 rpm should be minimum weight.

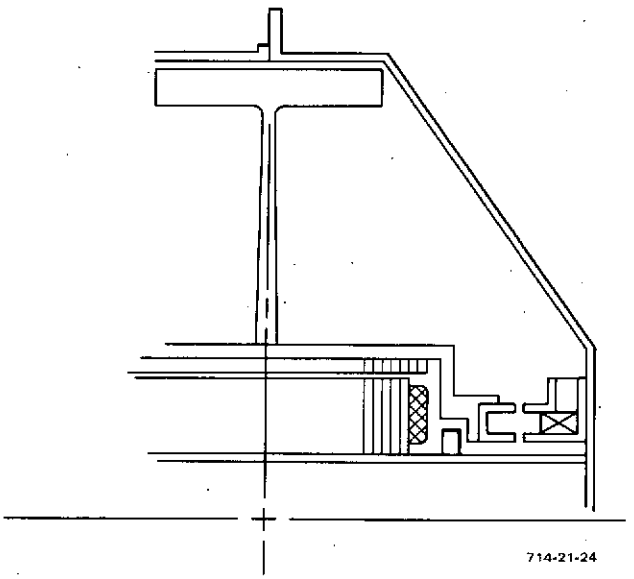

Figure 3-19
Conventional RWA Configuration

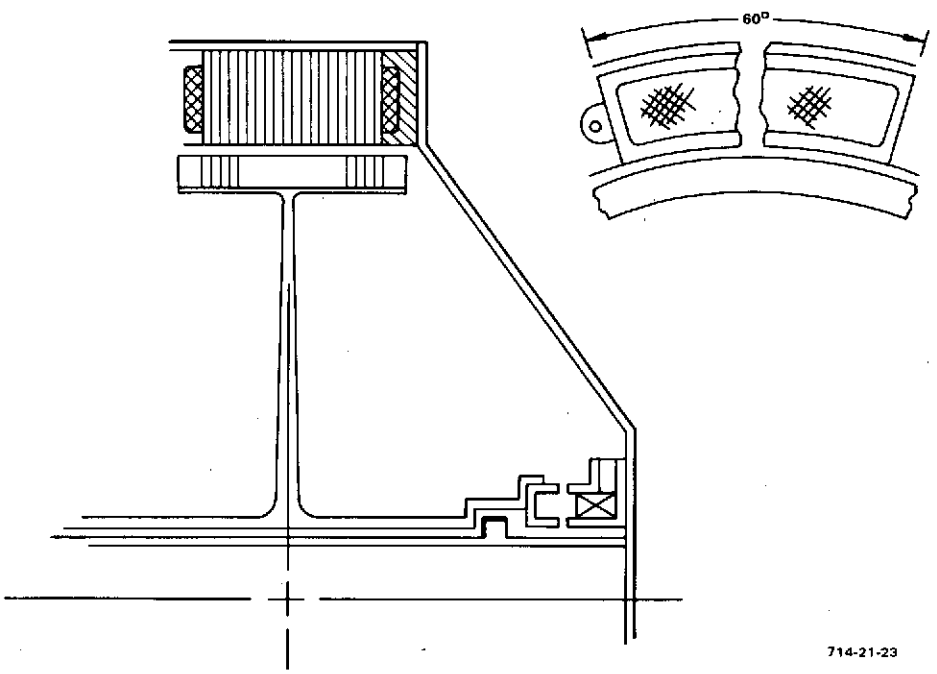

Figure 3-20
Segmented Motor Configuration

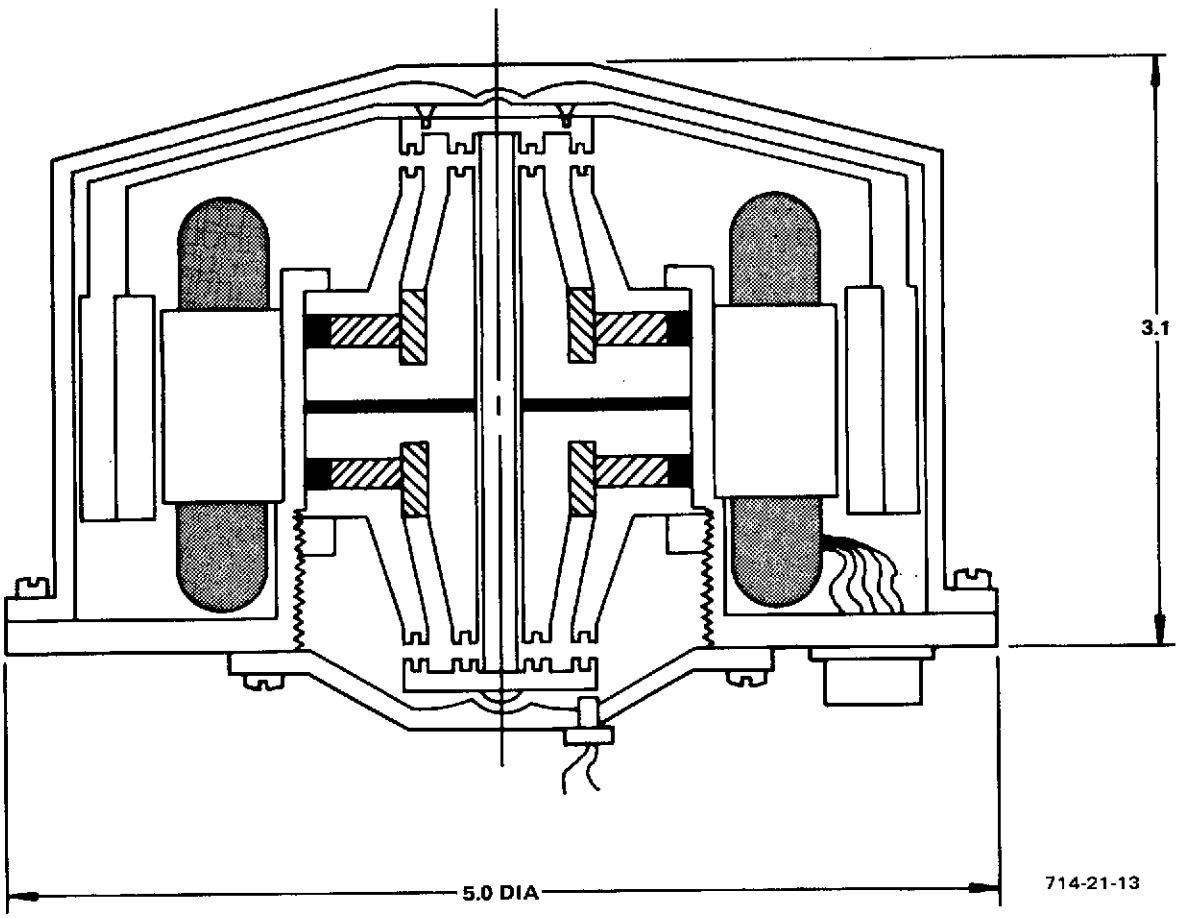

Figure 3-21
RWA Design Concept, Configuration A

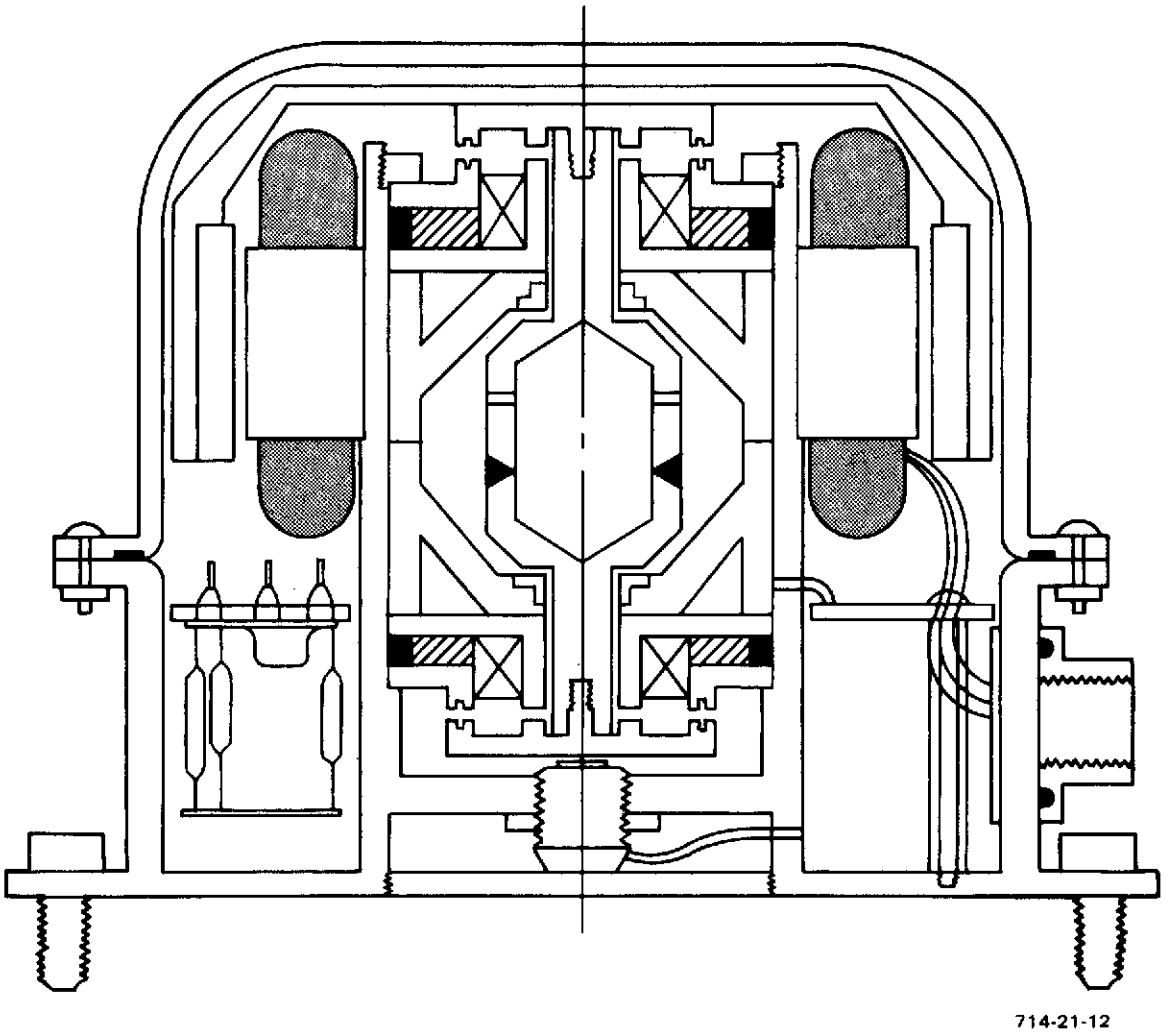

Figure 3-22
RWA Design Concept, Configuration B

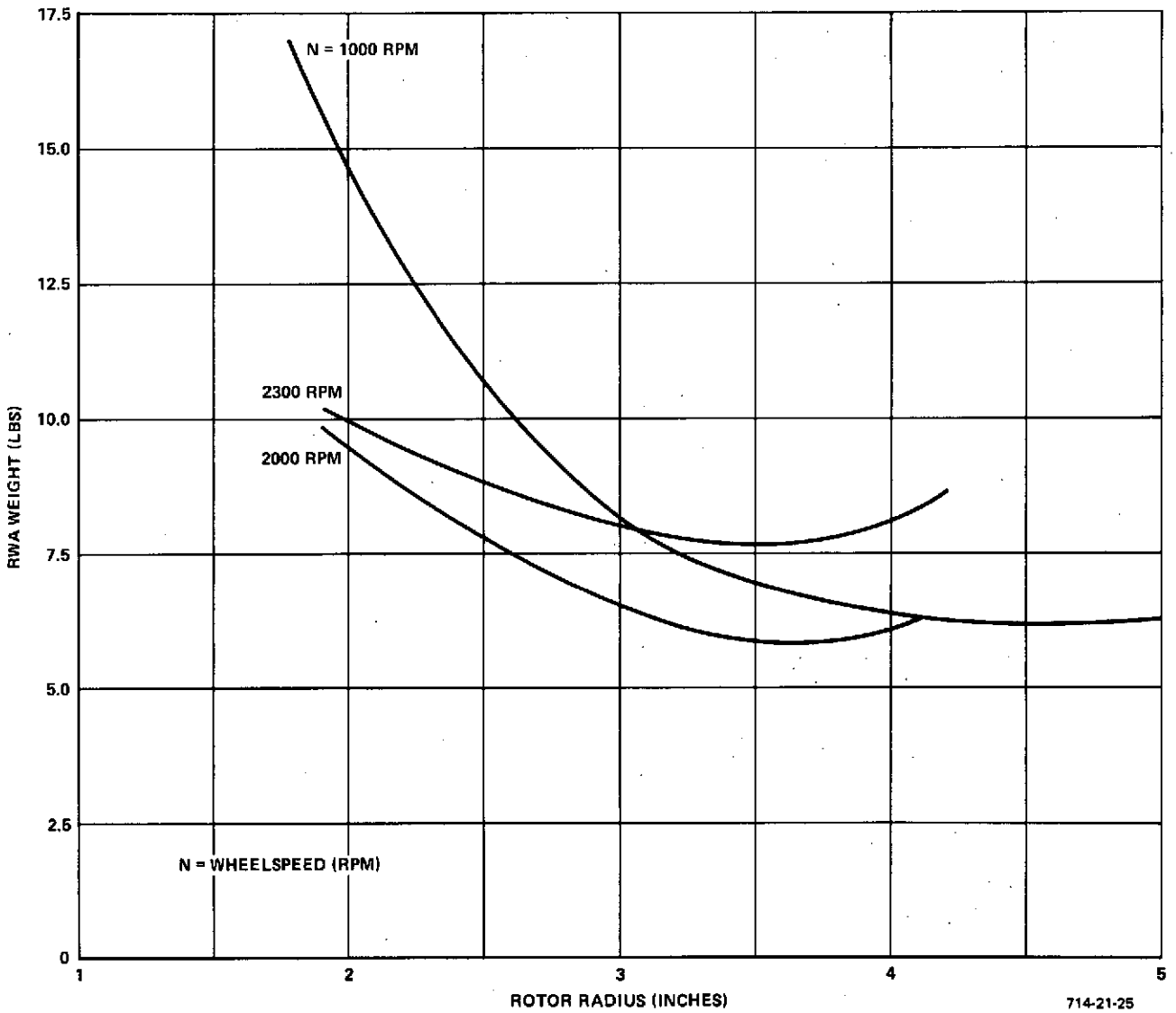

Figure 3-23
RWA Weight Versus Rotor Radius

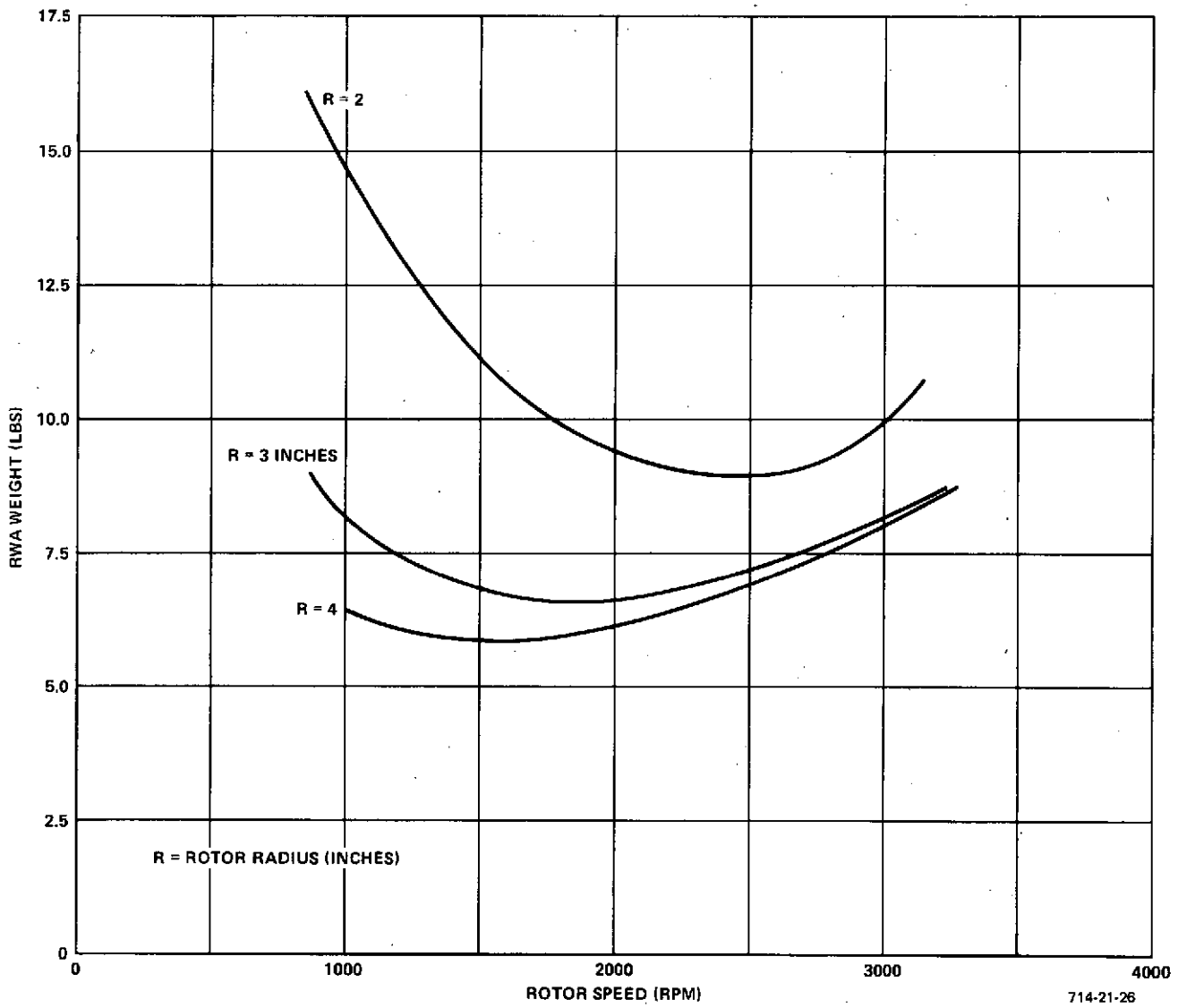

Figure 3-24
RWA Weight Versus Rotor Speed

Realizing that rotor weight and inertia vary with radius, and that motor configuration constraints do affect weight, a further tradeoff was made to determine the preferred motor. At the selected speed of 1500 rpm and 3.5 inch radius, one configuration utilizing a 360 degree, 2.0 inch radius motor was compared with a configuration using a segmented motor at 3.5 inch radius. The two configurations are shown schematically in Figures 3-25 and 3-26.

The weight comparison is as follows:

	2-inch motor radius	3.5-inch motor radius
Rotor	2.07	1.70
Stator	2.00	.60
Housing	2.52	2.84
Magnetic Suspension	.90	.90
	7.49 lb	6.04 lb

In addition to providing a weight advantage, the larger segmented motor provides the opportunity for a redundant spin motor, in addition to providing space for redundant bearing electronics and drive electronics if desired.

Based on a comparative evaluation of these design concepts, the segmented motor approach was selected wherein the motor cage serves as the prime inertial element. A preliminary layout of this concept is discussed in the following section.

3.4 PRELIMINARY DESIGN LAYOUT

The preliminary layout of the selected configuration is shown in Figure 3-27, which includes the segmented spin motor and the single loop magnetic suspension. The unit, as shown, is 8.9 inches in diameter and 4.6 inches high, and weighs 6.52 pounds.

The magnetic suspension configuration lends itself to the concept of machining after final assembly to establish the magnetic gaps and the touchdown system clearance. This approach is possible due to the mounting of the suspension system in a tube. The magnetic suspension elements are cylindrical in shape, stack inside the tube, and are secured by the nut at the upper end of the tube. The elements can be assembled in a fixture, which is a tube mounted on a base plate.

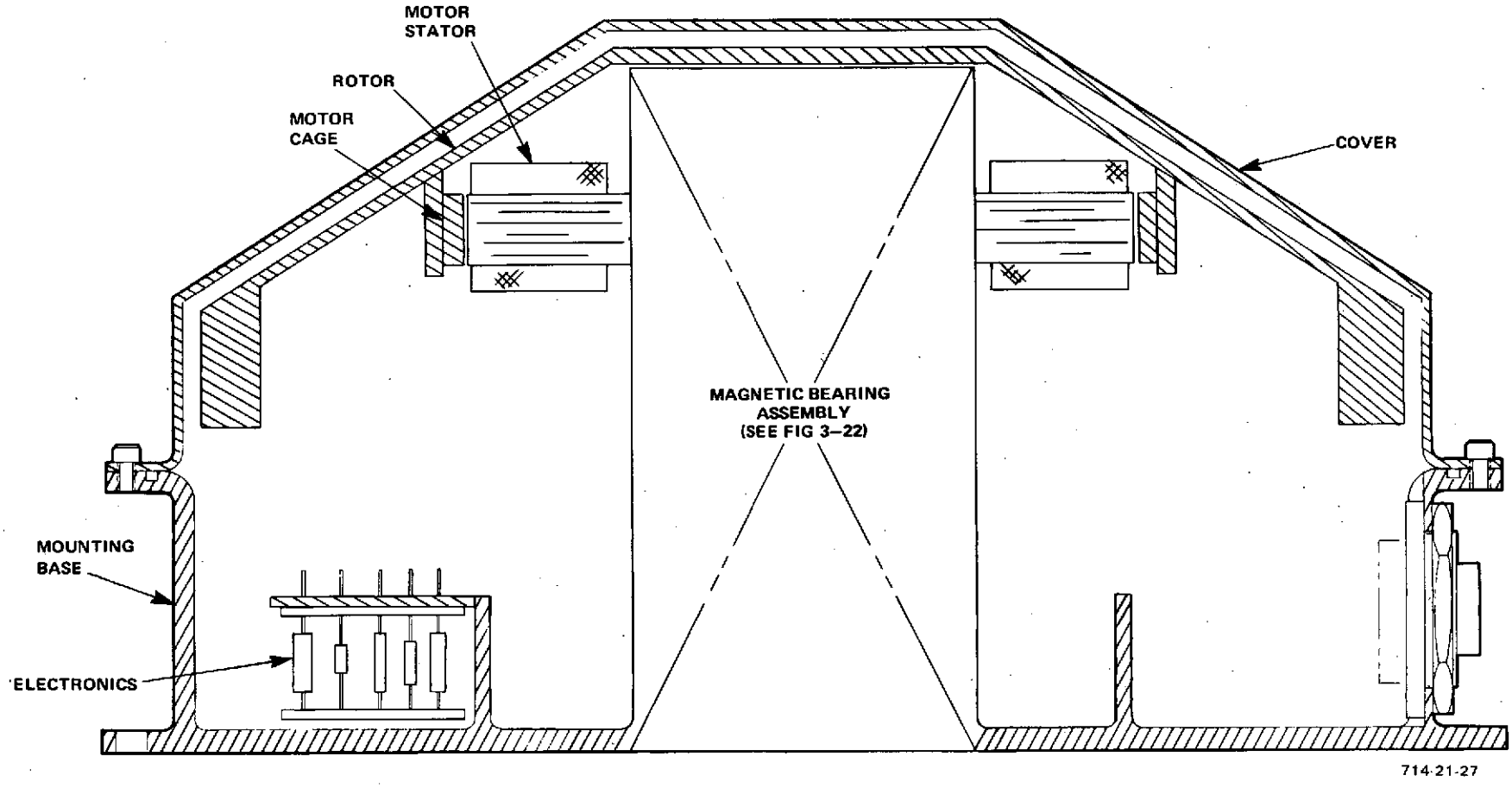

Figure 3-25
RWA Design Concept, Configuration C

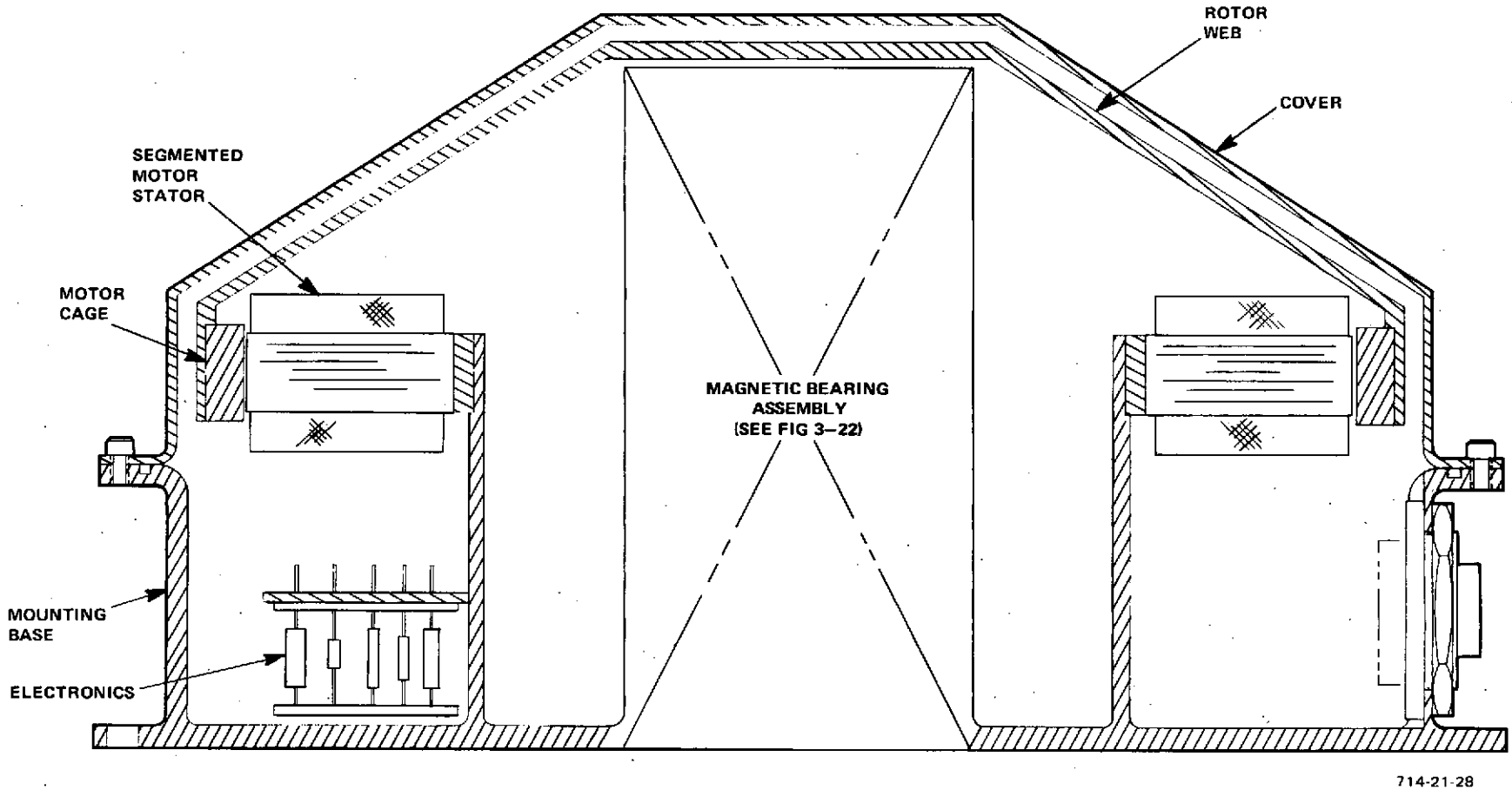

Figure 3-26
RWA Design Concept, Configuration D

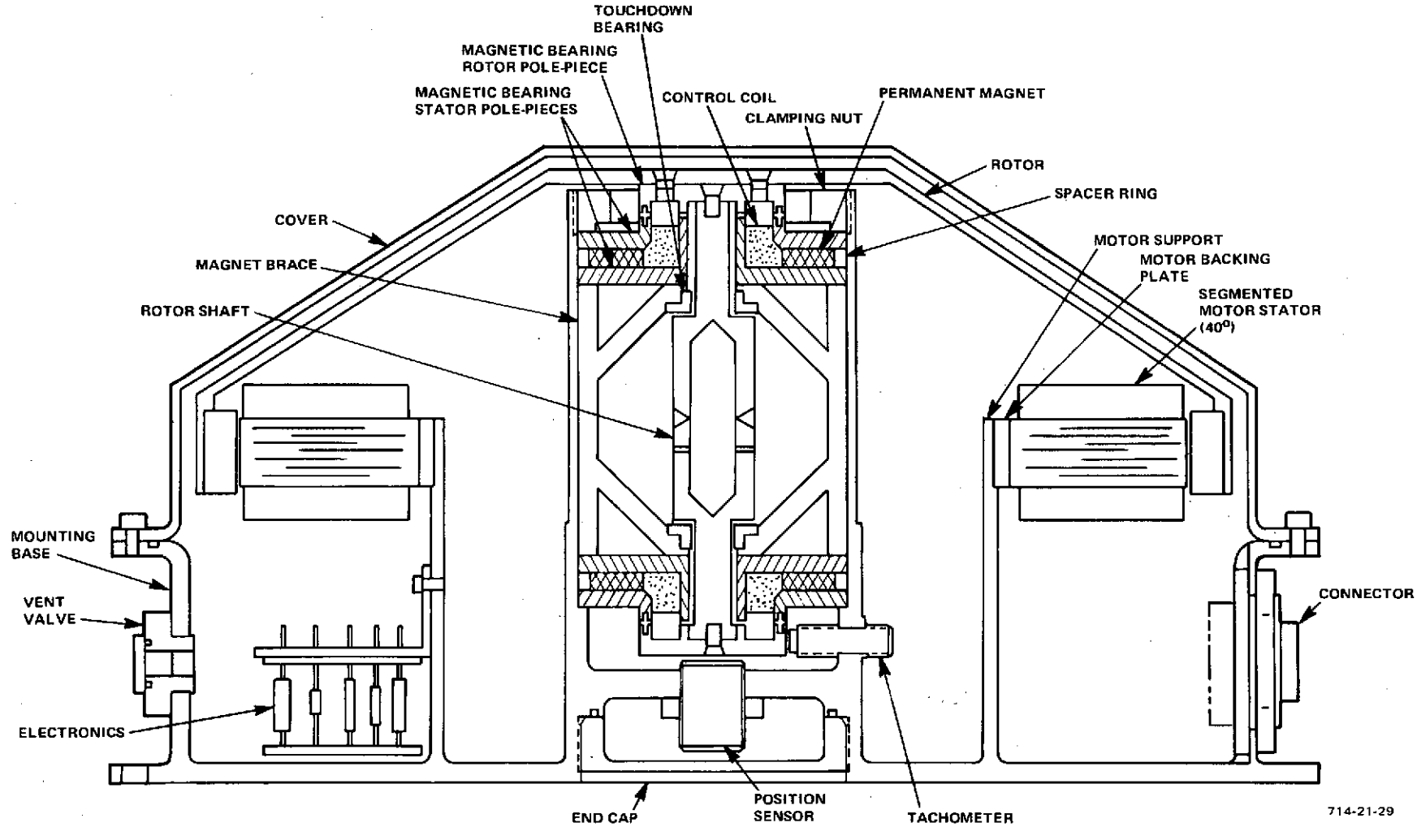

Figure 3-27
Preliminary RWA Design Layout

The tube is machined with access ports in the area of the lower magnetic gap, permitting measurement of the gap. A slot will be machined in the assembly tube in the axial direction to permit the angular alignment of the magnetic suspension elements during final assembly to minimize runout effects.

The layout is shown with a flush end mount to simplify the mechanical interface. A center of gravity mount would result in some weight savings, better utilization of the available volume, and potentially reduced vibration susceptibility.

The configuration also permits running of the unit without the cover which simplifies the instrumentation for calibration and test. The segmented spin motor provides the opportunity for adding a redundant motor stator without complicated redesign or any weight penalty other than the additional stator. The configuration also provides room for integral packaging of the suspension electronics, either single channel or redundant, and the spin motor drive electronics, if desired.

The preliminary layout (Figure 3-27) was used as the model for assessing the weight of the entire unit. The weight summary is listed in Table 3-5.

TABLE 3-5

MBRWA WEIGHT SUMMARY

Component	Weight (lb)
Housing	
Base	2.36
Cover	.55
Rotor	
Web	.90
Cage	1.00
Magnetic Suspension	.92
Motor Stator	.60
Electronics	.15
Connectors	.06
Vent Valve	.04
Electronics Mount	.02
Proximitor	.02
TOTAL	6.62

The materials used for assessing the weight of the unit were as follows:

Case/Cover	Aluminum alloy
Shaft	Titanium alloy
Web	Titanium alloy
Suspension spacers	Titanium alloy
Pole Pieces	Magnet iron

The detailed design process for the unit would consider the use of beryllium for the case/cover, shaft, and suspension spacers. In addition to effecting a weight reduction of approximately 1.3 pounds, the temperature sensitivity would also be reduced.

The tachometer shown in the layout is a simple variable reluctance pickup which was intended for use as a speed indicator for wheel unloading purposes. The vent valve is used to open the unit to the vacuum of space on orbit to prevent any buildup of pressure within the unit. This is desirable to maintain the predicted power levels over the 10 year life of the unit. Unlike ball bearing units, the magnetically suspended unit is not subject to lubricant loss problems, and thus can take full advantage of venting.

One feature of the design is the full containment of the permanent magnets, and the spacer ring between the pole pieces. These items eliminate the two major limitations of permanent magnets of this type, which are the presence of microcracks which could lead to particle generation and relatively low strength. The full containment feature of the design contains any particles, and the pole piece spacer removes mechanical load from the magnets.

It also should be noted that the design could be made without a cover. This is possible due to the restricted path available for admitting external contamination and no requirement for containing any lubricant. This feature would result in a unit weight of approximately 4.4 pounds when combined with the beryllium material substitution and a cg mount.

The preliminary design was based on a peak spin motor power of 8 watts and a momentum of ±.5 ft-lb-sec. If it is desired to reduce the spin motor power to 4 watts, this can be accomplished by increasing the motor stator weight and running the unit at the same speed or by increasing the rim weight and reducing the speed to one half of its present value. The motor efficiency is .278 at full speed with the present design, and it certainly could be increased to .56 by addition of more iron. Reducing the maximum speed to 750 rpm and increasing the rim weight by 1.2 pounds also effects a 4-watt reduction in power. This results in a sensitivity of no more than .3 pound per watt for a range of at least ±4 watts about the nominal 8-watt value.

SECTION 4.0

CONCLUSIONS

SECTION 4.0

CONCLUSIONS

This design study has resulted in the following conclusions concerning a magnetically suspended reaction wheel:

- The MBRWA is competitive with current ball bearing reaction wheels in terms of weight, power, and cost.
- The design completely eliminates all single point failure sources in a single mechanical assembly.
- The suspension electronics represents the only limitation of storage or operational life of the unit.
- The design eliminates the increase of spin motor power with low temperature and life that is encountered in ball bearing units.
- The magnetically suspended reaction wheel is much more tolerant to shock or vibration loading than a ball bearing unit because of the physical separation of the load carrying surfaces and the on orbit rotational suspension.
- The sensitivity of the design is

Spin motor peak power	.3 lb/watt
Suspension peak power	.025 lb/watt
Momentum	2.4 lb/ft-lb-sec
Redundant spin motor	.6 lb/motor

- The design configuration provides the opportunity for integral mounting of suspension and spin motor drive electronics, redundant spin motor, and inherently provides redundant suspension coils.
- The design weight can be reduced to 4.4 pounds by use of selected materials and the elimination of the cover, which is not required on orbit.
- The MBRWA design which resulted from the study meets the design objectives set forth in the Statement of Work. The major design objectives and the resulting performance are listed in Table 4-1.

TABLE 4-1

MAJOR DESIGN OBJECTIVES

Parameter	Design Objectives	Attained Value
Angular Momentum	±.5 ft-lb-sec	±.5 ft-lb-sec
Weight	8.0 lb	6.62 lb
Size	250 in.	220 $in.^3$ (8.9 in. diameter x 4.6 in. high)
Cross Axis Rate	17.5 mr/sec	832 mr/sec
Output Torque	.01 ft-lb	.01 ft-lb
Motor Power (maximum)	8 watts	8 watts
Bearing Power		
Maximum	8 watts	8 watts
Average	1 watt	.5 watt

SECTION 5.0

RECOMMENDATIONS

SECTION 5.0

RECOMMENDATIONS

Based on the conclusions presented in Section 4.0, it is recommended that a hardware development program be initiated for a magnetically suspended RWA. This program would be composed of two phases, leading eventually to a qualified flight model. The first program phase is an engineering development, based on the presently recommended design approach, and would result in an engineering model suitable for functional and environmental testing. At the completion of this development effort, a flight unit would be designed and qualified to a detailed equipment specification.

A program plan for RWA development (Phase I) is presented in the remainder of this section, and consists of detail task descriptions and a program schedule (Figure 5-1). The duration of this development program is 12 months, and it is estimated that the follow-on flight qualification (Phase II) would require an additional 18 months.

TASK DESCRIPTIONS

1.0 Preliminary Design Requirements

Outline of RWA design requirements, based on the specified performance, interface and environmental requirements of the intended application.

2.0 Design Analyses

Based on the results of Task 1, detail design analyses will be prepared to establish the critical component parameters. Preliminary estimates of RWA weight and power will also be made.

3.0 Component Development Tests

These tests comprise those necessary to verify the design approach in certain areas; principal among these is the operability of the touchdown system.

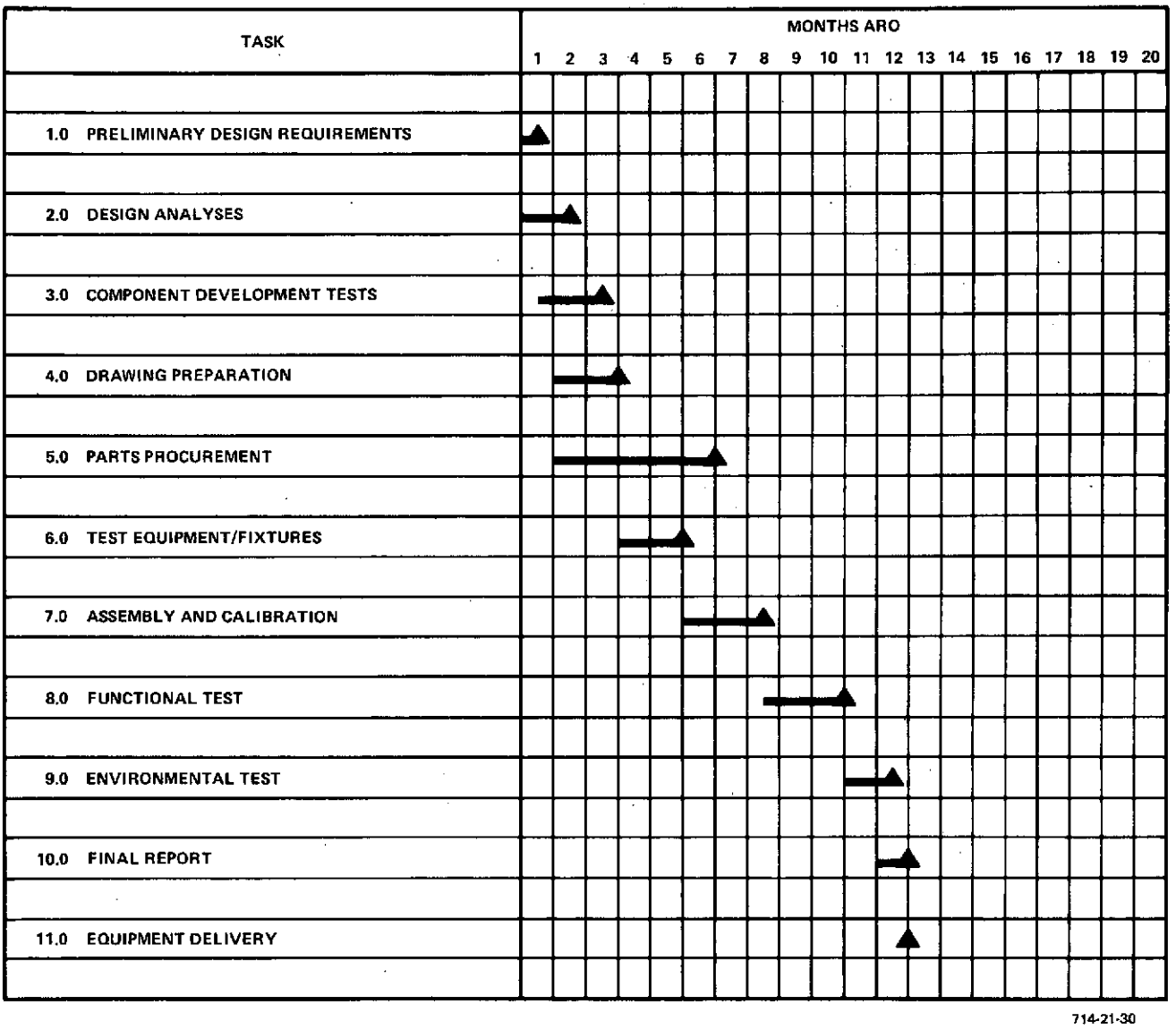

Figure 5-1
RWA Development Schedule, Phase I

4.0 Drawing Preparation

A layout will be made from which detail drawings can be prepared for parts procurement and/or fabrication. Final weight calculations will be made from these drawings.

5.0 Parts Procurement

Parts will be procured for the engineering model. The spin motor is expected to be the only long lead item, and its development will be coordinated with a vendor during the design analysis task.

6.0 Test Equipment and Fixtures

Special test equipment and holding fixtures will be designed and fabricated.

7.0 Assembly and Calibration

Assembly and calibration of the RWA, including component performance data verification, wheel dynamic balance and bearing control system evaluation.

8.0 Functional Test

Testing of the RWA to evaluate operability and performance. Major parameters of interest are power (transient and steady state), drag torques, cross axis rates, rotor/bearing dynamics, touchdown system and spin motor performance.

9.0 Environmental Test

Measurement of performance under thermal vacuum exposure; sinusoidal vibration survey to determine primary resonances; random vibration exposure.

10. Final Report

Description of development results, with recommendations for flight hardware design.

11.0 Equipment Delivery

Refurbishment (as required) and delivery for test at JPL.

SECTION 6.0

NEW TECHNOLOGY

SECTION 6.0

NEW TECHNOLOGY

The technical information contained in this report is based on prior developments at Sperry Flight Systems, in the areas of reaction wheel assemblies, motors and magnetic bearings. There was no new technology developed during the course of this contract.

APPENDIX A

DESCRIPTION OF THE SPERRY MAGNETIC BEARING MODEL

APPENDIX A

DESCRIPTION OF THE SPERRY MAGNETIC BEARING MODEL

The Sperry magnetic bearing model, which uses a unique three-loop design, is described in this appendix. The purpose is to provide background data, developed prior to this present JPL study effort, which substantiates certain decisions made during the course of the RWA design as described in Section 3.0 of this report. The results are especially applicable because the bearing radial stiffness is nearly the same as required in the .5 ft-lb-sec RWA. A photograph of this model is shown in Figure A-1.

A.1 PHYSICAL DESCRIPTION

The magnetic bearing model was constructed in order to verify design approaches and to obtain test data prior to application of magnetic bearings to a large (700 ft-lb-sec) reaction wheel assembly. The cross-section of each individual bearing is shown in Figure A-2.

The model consists of a shaft mounted on two magnetic bearings, with preloaded ball-bearings at each shaft end provided for touchdown during shaft rotations. An ac induction motor is used for application of torque about the spin axis. Samarium-cobalt magnets establish a quiescent flux between axially opposed soft iron rings, this flux being modulated by the control coils to provide axial control forces. Radial damping is provided by copper wires which are cemented in the pole-face grooves at the magnetic gaps. The axial control system utilizes a single lead-lag network for compensation, with a current amplifier to drive the coils. Provisions were made for test with or without the positive integral feedback technique (Paragraph 3.2.3). Eddy-current proximeters are used both for axial position sensing, as well as for monitoring radial displacements.

A.2 TEST RESULTS

The test model has been successfully levitated and rotated at speeds up to 11,500 rpm, both in air and under evacuated conditions. Successful operation of the ball bearing touchdown system has also been achieved over this speed range. Very stable suspension has been attained, with minimal power loss under both ambient conditions and steady external loads achieved with the use of positive integral feedback of control current.

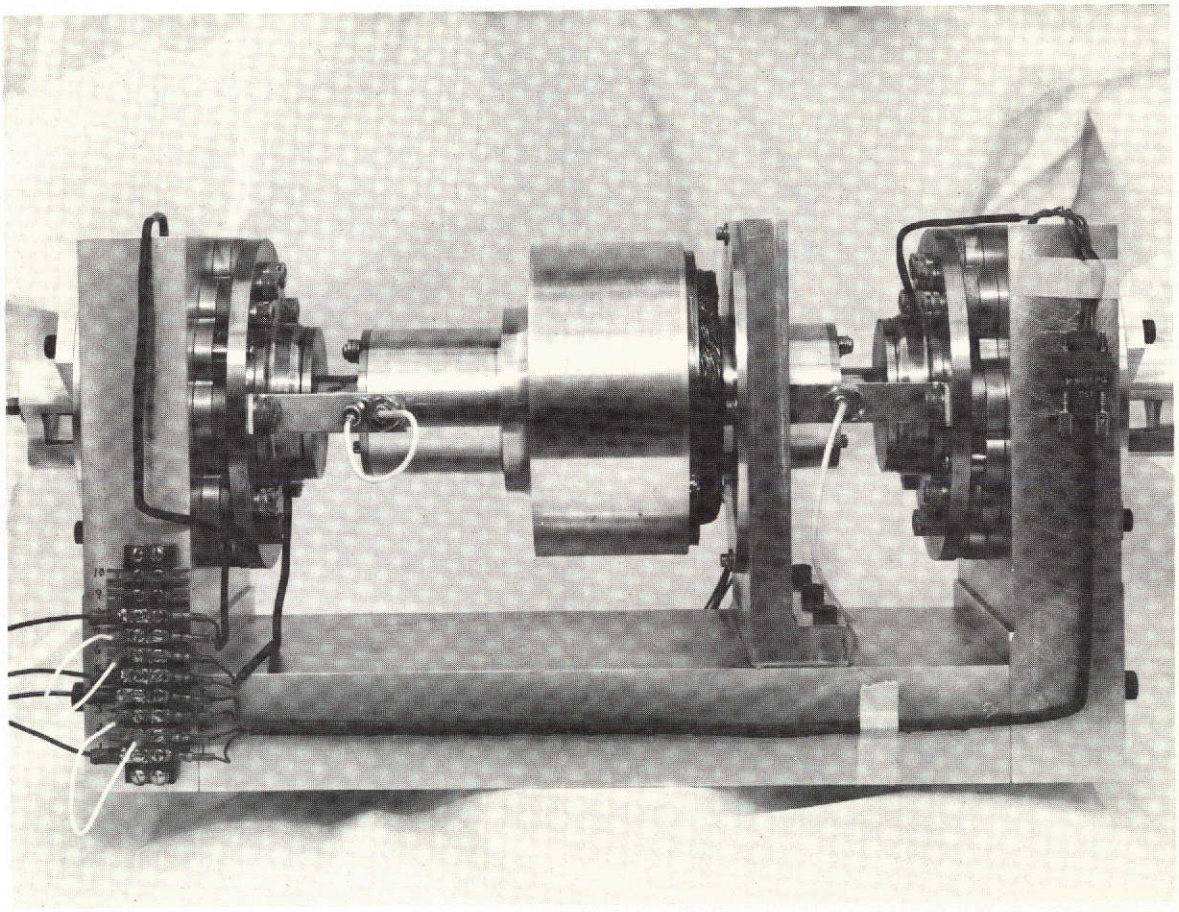

714-21-8

Figure A-1
Magnetic Bearing Model

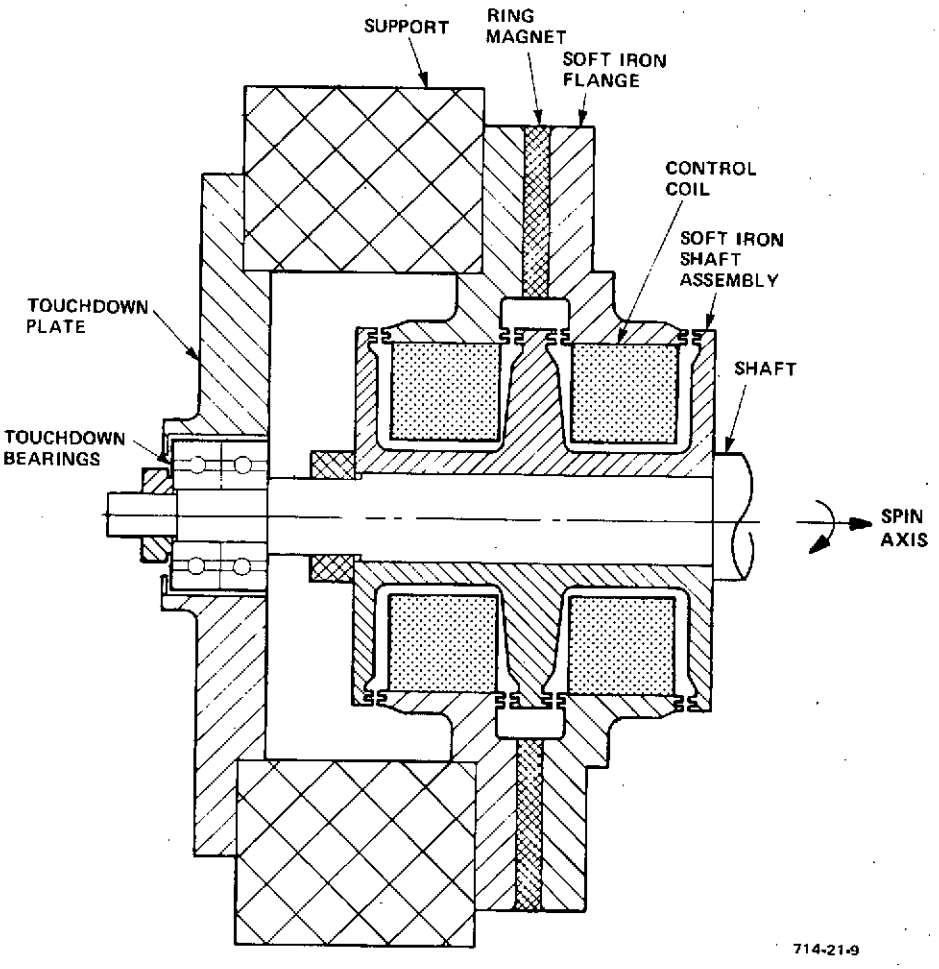

Figure A-2
Magnetic Bearing Sectional View

The measured bearing model characteristics were:

- Drag torque coefficient — .01 oz-in./1000 rpm
- Stiffness
  - Radial (single bearing (K_r) — 165 lb/in.
  - Axial (net) — 2000 lb/in. (controllable)
  - Axial Unbalance (K_u) — -2400 lb/in.
- Capacity
  - Radial Touchdown — 7 lb
  - Axial Touchdown — 25 lb
- Gap Flux Density — ~ 4300 gauss (average)
- Touchdown Gap
  - Radial — .025 in.
  - Axial — .012 in.
- Axial Magnetic Gap — .020 in.
- Rotor Weight — 4.5 lb
- Control System Power — < 1 watt (electronics)
  (with integrator) — 0 (control coils)

Drag torque measurements were made over the range of 0 to 4000 rpm. The measured coefficient of .1 oz-in./1000 rpm is due to eddy current effects, and is expected to be constant over a large speed range. The breakaway torque, which is due to hysteresis effects in the pole pieces and magnetic non-uniformities, was measured at less than .005 oz-in.

The measured radial stiffness is shown in Figure A-3, and agrees extremely well with stiffness predicted from complex variable analyses. Note that this characteristic is almost linear over .015 inch, which is the thickness of each ring on the pole faces.

The axial stiffness curves are shown in Figure A-4. Stable, zero-current operation was possible with the displacement and derived-rate feedback control for a large range of feedback gains. The axial stiffness and damping were continuously adjustable. It was possible to operate from all four coils simultaneously, or from two coils in a single bearing at a time. The frequency response was in good agreement with analysis, and it was found that the maximum gain before instability was dependent on amplifier saturation.

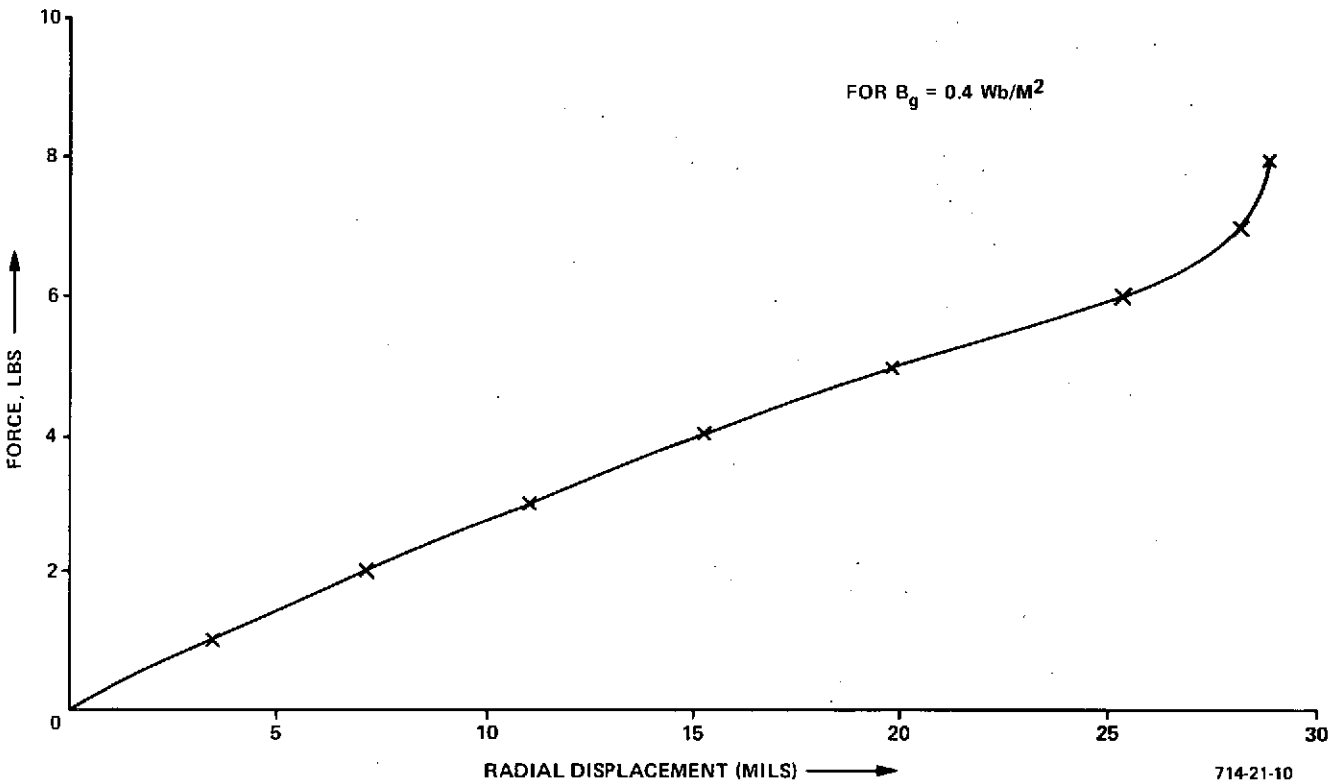

Figure A-3
Measured Radial Stiffness (K_N)

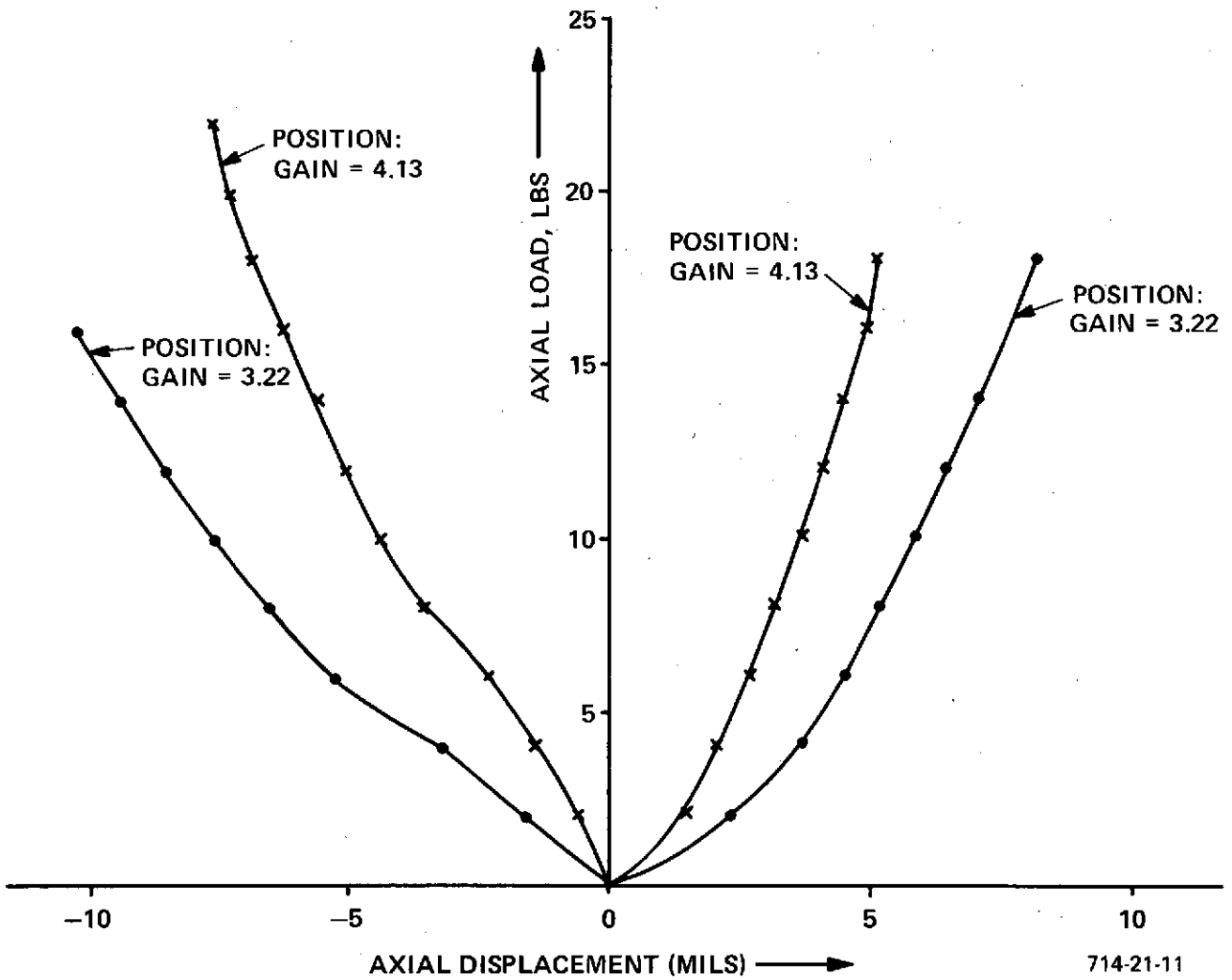

Figure A-4
Measured Axial Stiffness

The addition of integral feedback resulted in zero-current operation with the axis vertical with the resultant negative stiffness observable.

Both the axial and radial responses to step forces (or displacement conditions) were found to be well damped. The axial response could be varied by adjusting rate gain.